Characterization of genomic variants associated with resistance to bedaquiline and delamanid in naïve *Mycobacterium tuberculosis* clinical strains

Battaglia S[a], Spitaleri A[a,b], Cabibbe AM[a], Meehan CJ[c,d], Utpatel C[e], Ismail N[f], Tahseen S[g], Skrahina A[h], Alikhanova N[i], Kamal SM Mostofa[j], Barbova A[k], Niemann S[e, l], Groenheit R[m], Dean AS[n], Zignol M[n], Rigouts L[d,o], Cirillo DM[a#]

[a] Emerging Bacterial Pathogens Unit, Division of Immunology, Transplantation and Infectious Diseases, IRCCS San Raffaele Scientific Institute, Milan, Italy

[b] Center for Omics Sciences, IRCCS San Raffaele Scientific Institute, Milan, Italy.

[c] School of Chemistry and Biosciences, University of Bradford, Bradford, UK.

[d] Unit of Mycobacteriology, Department of Biomedical Sciences, Institute of Tropical Medicine, Antwerp, Belgium.

[e] Molecular and Experimental Mycobacteriology, Research Center Borstel, Borstel, Germany.

[f] Centre for Tuberculosis, National Institute for Communicable Diseases, National Health Laboratory Services, Johannesburg, South Africa.

[g] National TB Reference Laboratory, National Tuberculosis Control Program, Islamabad, Pakistan.

[h] Republic Research and Practical Centre for Pulmonology and Tuberculosis, Minsk, Belarus.

[i] Scientific Research Institute of Lung Diseases, Ministry of Health, Baku, Azerbaijan.

[j] National TB Reference Laboratory, National Institute of Diseases of the Chest and Hospital, Dhaka, Bangladesh.

[k] Central Reference Laboratory on Tuberculosis Microbiological Diagnostics, Ministry of Health, Kiev, Ukraine.

[l] German Center for Infection Research (DZIF), Partner Site Hamburg-Lübeck-Borstel-Riems, Germany.

[m] Unit for Laboratory Surveillance of Bacterial Pathogens, Public Health Agency of Sweden, Solna, Sweden.

[n] Global TB Programme, World Health Organization, Geneva, Switzerland.

[o] Department Biomedical Sciences, Antwerp University, Antwerp, Belgium.

Running title: Markers of resistance to bedaquiline and delamanid.

Address correspondence to Daniela Maria Cirillo, PhD, MD: cirillo.daniela@hsr.it

Abstract

The role of genetic mutations in genes associated to phenotypic resistance to bedaquiline (BDQ) and delamanid (DLM) in *Mycobacterium tuberculosis* complex (MTBc) strains is poorly understood. However, a clear understanding of the role of each genetic variant is crucial to guide the development of molecular-based drug susceptibility testing (DST). In this work, we analysed all mutations in candidate genomic regions associated with BDQ- and DLM-resistant phenotypes using a whole genome sequencing (WGS) dataset from a collection of 4795 MTBc clinical isolates from six high-burden countries of tuberculosis (TB). From WGS analysis, we identified 61 and 158 unique mutations in genomic regions potentially involved in BDQ- and DLM-resistant phenotypes, respectively. Importantly, all strains were isolated from patients who likely have never been exposed to the medicines. In order to characterize the role of mutations, we performed an energetic *in silico* analysis to evaluate their effect in the available protein structures Ddn (DLM), Fgd1 (DLM) and Rv0678 (BDQ), and minimum inhibitory concentration (MIC) assays on a subset of MTBc strains carrying mutations to assess their phenotypic effect. The combination of structural protein information and phenotypic data allowed for cataloging the mutations clearly associated with resistance to BDQ (*n*= 4) and DLM (*n*= 35), as well as about a hundred

genetic variants without any correlation with resistance. Importantly, these results show that both BDQ and DLM resistance-related mutations are diverse and distributed across the entire region of each gene target, which is of critical importance to the development of comprehensive molecular diagnostic tools.

Importance

Phenotypic drug susceptibility tests (DST) are too slow to provide an early indication of drug susceptibility status at the time of treatment initiation and very demanding in terms of specimens handling and biosafety. The development of molecular assays to detect resistance to bedaquiline (BDQ) and delamanid (DLM) requires accurate categorization of genetic variants according to their association with phenotypic resistance. We have evaluated a large multi-country set of clinical isolates to identify mutations associated with increased minimum inhibitory concentrations (MICs) and used an *in silico* protein structure analysis to further unravel the potential role of these mutations in drug resistance mechanisms. The results of this study are an important source of information for the development of molecular diagnostic tests to improve the provision of appropriate treatment and care to TB patients.

1. Introduction

The management of drug resistant tuberculosis (DR-TB) caused by *Mycobacterium tuberculosis* complex (MTBc) strains poses a serious public health challenge worldwide. The World Health Organization (WHO) new guidelines recommend the use of bedaquiline (BDQ) for all TB cases of rifampicin resistance (RR-TB), multi drug resistant (MDR) TB (MTBc strains resistant at least to isoniazid and rifampicin) and extensively drug-resistant (XDR) TB (MDR strains resistant to fluoroquinolones and second-line injectables drugs) (**1**). Based on WHO priority grouping of medicines, Delamanid (DLM) compound is recommended when an effective regimen cannot be established by group A agents,

containing BDQ, fluoroquinolones (FQs), linezolid (LZD) and B agents group, composed by clofazimine (CLF) and cycloserine (CS) (**2**). Previous studies have shown that MDR/XDR-TB patients treated with BDQ and DLM rapidly develop resistance due to fixed mutations in candidate genes which often appear as previously undescribed novel variants (**3, 4, 5, 6, 7**). Additionally, resistance to BDQ can arise in naïve populations of MTBc strains as a consequence of a clofazimine-containing regimen, or by random mutations affecting the drug targets (**8, 9, 10, 11, 12, 13, 14**). DLM resistance not associated to exposure has been reported as well (**15, 16, 17, 18, 19**). Moreover, as a member of the nitroimidazooxazines, DLM shares the same resistance mechanisms of pretomanid (PA-824) compound (**20**).

Therefore, knowledge of the BDQ and DLM susceptibility status of clinical MTBc isolates before therapy has started and the early detection of emerging resistance in failing regimens are needed to ensure an effective treatment of DR-TB.

Here, whole genome sequencing (WGS) based approaches, that are rapidly expanding from basic research into routine diagnostic laboratories, provide the advantage of interrogate virtually all resistance targets in a given clinical MTBc strain. However, the routing diagnostic application of WGS requires a much better understanding of the correlation between genotypic and phenotypic, particularly for the new drugs (**21, 22**).

Currently, the molecular mechanisms leading to resistance to BDQ and DLM are not well described, a fact that jeopardises the design of a reliable molecular approach to detect resistance.

Mutations in *atpE* (*Rv1305*), which encodes for the C-subunit of ATP synthase, have been associated with phenotypic resistance to BDQ, which is known to directly inhibit the ATP synthase (on target mechanism) (**23**). In addition, the mutations in the off-target *Rv0687* gene result in increased minimum inhibitory concentrations (MICs) for BDQ by up-

regulation of the MmpL5/MmpS5 pump gene expression, concurrently leading to a cross-resistance to clofazimine (CLF) (**10, 11, 24**). Furthermore, it has been demonstrated that mutations in *pepQ* (*Rv2535c*) may confer low-level resistance to both CLF and BDQ in clinical isolates (**9, 25**).

DLM impairs the biosynthesis of mycolic acids and requires activation by the F420-dependent nitroreductase encoded by the *ddn* gene (on target mechanism). The F420 cofactor is synthetized by enzymes encoded by the *fbiA, fbiB, fbiC, fgd1* genes, all of which are involved in DLM off-target mechanisms. Polymorphisms in these genes were shown to be involved in phenotypic DLM resistance (**26, 27**).

To better describe BDQ and DLM resistance mechanisms, we investigated the genomic regions involved in resistance to BDQ and DLM from 4795 MTBc isolates collected within a multi-country drug-resistance surveillance study and to identify variants potentially involved in resistance development (**28**). The mutations found were correlated with strain lineage, DR-profile and country of origin. To combine the genomic data with phenotypes, we performed BDQ and DLM MICs for a subset of these isolates. Finally, for the available 3D protein structures (Ddn, Fgd1 and Rv0678) we performed an *in silico* structural and energetic analysis in order to characterize and quantify the mutation effect on protein function. This combined information enabled us to provide a first robust catalogue of BDQ and DLM resistance mutations as basis of the establishment of WGS resistance prediction algorithms for these drugs.

2. Methods

2.1 Study design

A total of 4795 genome sequences retrieved from the Sequence Read Archive of the National Center for Biotechnology Information as recalibrated BAM files (accession number SRP128089) were considered and investigated in this study. The corresponding

MTBc isolates originate from a unique population-based surveillance study across six countries with a high burden of TB or MDR-TB, according to WHO's high burden country list for the period of 2016-2020: Azerbaijan (*n* = 751), Belarus (*n* = 197), Bangladesh (*n* = 935), Pakistan (*n* = 194), South Africa (*n* = 1578), Ukraine (*n* = 1140) (**28**). For our purposes, all sequenced isolates harbouring at least one single nucleotide polymorphism (SNP) or insertion/deletion (indel) in at least one of the candidate genomic regions for DLM and/or BDQ resistance were considered for the analysis, excluding synonymous mutations and previously characterized lineage-associated SNPs for which the absence of correlation with the phenotypic DLM resistance was demonstrated (**15, 16**). For genetic variants detected in more than one isolate we decided to replicate results selecting two isolates from different countries, whenever possible. The flowchart for sample selection, the number of isolate tested and phenotypic drug-susceptibility testing (DST) of selected isolates are reported in Figure S1 of supplementary materials.

2.2 Whole Genome Sequencing analysis

WGS data were generated by both Illumina technology (Illumina, San Diego, CA, USA) and Ion Torrent technology (ThermoFisher Scientific) as previously described (**28**). Sequencing data were analysed using the MTBseq pipeline (**29**) to identify all variants in the genomes and MTBc lineage. The analysis was performed on the mapped MTBc reads by setting a quality threshold of at least a mean coverage of 20x and an unambiguous base call threshold of ≥70%. A mutation was called only if SNPs and/or indel variants were detected by at least eight reads (both forward and reverse reads) with a minimum phred quality score of 20, and by considering a mutation frequency of ≥75%. The regions of the MTBc genome reference H37Rv NC_000962.3 (**30**) considered in the study are reported in Table S1 of supplementary materials. The WGS analysis results and distribution of

mutations among lineages and countries of isolation are reported in the supplementary excel Dataset S1.

Cluster analysis was performed on the distance matrix generated by the MTBseq pipeline using *in-house* python scripts (https://github.com/aspitaleri/python). The distance matrix was analysed using a hierarchical linkage clustering method with a 12 SNPs cut-off (**31**).

2.3 Minimum Inhibitory Concentration assay

The selected MTBc isolates for genetic variants were sub-cultured on Löwenstein-Jensen medium and subsequently subjected to MIC testing against BDQ and/or DLM by the resazurin colorimetric microtiter plate assay (REMA) as previously described (**16, 32, 33**). Delamanid powder was obtained from Otsuka Pharmaceutical (Tokyo, Japan) and pure bedaquiline powder was obtained from Janssen Pharmaceutical (Beerse, Belgium). A DLM concentration range of 0.004-4 µg/ml and a BDQ concentration range of 0.004-2 µg/ml were used, considering the proposed cut-off values of 0.12 µg/ml and 0.06 for BDQ and DLM, respectively (**34**). Based on MIC results, the isolates were categorized as susceptible (S; MIC ≤ cut-off), low resistant level (I; MIC 1 dilution > cut-off) or resistant (R; MIC more than 1 dilution > cut-off). All MIC values reported in this work correspond to the MIC100 value that considers any change in colour to purple/pink as indicating the presence of viable bacilli (**33**). For each batch of isolates tested, the H37Rv *M. tuberculosis* reference strain (*M. tuberculosis* H37Rv ATCC 27294) was included as a control, and test isolate results of that batch were accepted only if the H37Rv MIC value was within the expected range of ≤0.004-0.03 µg/ml for DLM and ≤0.008-0.03 µg/ml for BDQ. Further details of REMA protocols are reported in supplementary materials Text S1 word file.

2.4 Mutation structural analysis

We carried out an energetic analysis on the available crystal structures of proteins Ddn (PDB 3R5R), Fgd1 (PDB 3B4Y) and Rv0678 (PDB 4NB5) (**35, 36, 37**) using Eris (**38**) and MAESTRO (**39**) programs. We exploited two end-point methods to evaluate the change of protein stability upon mutations, namely Eris and MAESTRO, which calculate the folding free energy in two different manners. For this structural analysis stop codons, frameshifts, and SNPs affecting the promoter region were not included. The stability change, $\Delta\Delta G$, is computed as the difference between the average stabilities of mutant and wild type protein structures. Both *in silico* approaches were used as a qualitative cross-validation to evaluate the protein mutation effects, considering 0.34 Kcal/mol and 5 Kcal/mol as thresholds for MAESTRO and Eris, respectively.

In addition to folding stability, we calculated the effect of mutations on the complex stabilities Ddn-F420-H_2 Fgd1-F420-H_2 using DSX pair potentials knowledge-based scoring function (**40**). In case of Rv0678 protein we also performed an energetic analysis to quantify the effect of the mutations on the homodimer protein-protein stability. For this purpose, we carried out a molecular mechanics energies combined with the Generalized Born and surface area continuum solvation (MM/GBSA). The calculation was performed using MMPBSA.py program within Amber14 suite using ff14 force field and the GB^{OBC1} implicit solvent model (**41**). All obtained *in silico* results are reported in the supplementary material Dataset S2. Further details of *in silico* analyses are reported in supplementary materials Text S1 word file. Primary protein sequences alignment for the frameshift analysis was performed using ClustalX algorithm (**42**). The visualization of the mapped mutations on the protein structures are created with PyMOL v2.0 (**43**).

3. Results

A total of 4795 WGS from MTBc clinical strains were analysed by considering the candidate genomic regions for BDQ resistance (*atpE, Rv0678, pepQ*) and for DLM

198 resistance (*ddn, fgd1, fbiA, fbiB, fbiC*). This collection included 731 (17%) MDR and 79
199 (2%) XDR MTBc strains (Fig. S1). Based on WGS results, we identified a total of 106 and
200 643 isolates harboring relevant genomic variants potentially involved in BDQ and DLM
201 resistance, respectively. We tested a subset of isolates carrying mutations for phenotypic
202 DST for BDQ (*n*= 51) and for DLM (*n*= 124) representing the 43 and 104 BDQ- and DLM-
203 related variants, respectively (Fig. S1). All genomic variants detected by WGS analysis in
204 candidate genes for BDQ and DLM with the corresponding information of MTBc strain
205 lineage, drug resistance profile, country of isolation, mutation frequency and MIC results
206 for tested MTBc isolates are reported in Dataset S1 of supplementary material.

207 ***3.1. Analysis of mutations for BDQ resistance***

208 The WGS analysis revealed 61 unique mutations in the considered genomic regions
209 associated with BDQ resistance (Fig. S1). The mutation analysis distribution revealed 27
210 unique mutations in *Rv0678* (including 7 mutations in the promoter region, 16
211 nonsynonymous mutations, and 4 indels causing frameshift mutations), 32 unique
212 mutations in the *pepQ* gene (including 2 upstream mutations, 28 nonsynonymous
213 mutations and 2 frameshift mutations), and 2 upstream mutations in the *atpE* gene, while
214 no mutations were found in the *atpE* encoding region (Dataset S1).

215 Phenotypic testing revealed that four different *Rv0678* mutations had MIC values above
216 the cut-off of 0.12 µg/ml: two frameshift (fs) mutations in *Rv0678*, Gly6fs (del_16-17 gg)
217 and the double mutant Gln9fs-Thr92fs (ins_27 c, ins_274 a) associated with an MIC of 0.5
218 µg/ml, and two *Rv0678* nonsynonymous mutations Arg96Trp and Met111Lys yielding a
219 low level of resistance to BDQ of 0.25 µg/ml (Table 1). The two frameshift mutations
220 associated with BDQ-resistant phenotypes were observed in one MDR isolate and another
221 MDR isolate with concurrent resistance to FQs (corresponding to one new and one

222 previously treated TB case, respectively). Two nonsynonymous mutations associated to
223 low level resistance were found in two pan-susceptible (full-S) MTBc strains (Table 1).
224 The other 39 mutations were detected in isolates susceptible to BDQ with MIC values
225 ≤0.12 µg/ml, including two isolates harbouring frameshifts in Rv0678: Ile16fs (ins_ 46
226 tcatggaattcg) and Ala153fs (ins_457 c) showing an MIC of 0.06 µg/ml. (Dataset S1). The
227 protein amino acid sequences obtained from these two frameshifts mutations were aligned
228 to the Rv0678 wild-type sequence, highlighting that both wild-type and mutated proteins
229 contain the two well-conserved and important regions: the amino acid (aa) positions from
230 34 to 99 (DNA-binding domain) and positions from 16 to 32 and from 101 to 160
231 (dimerization domains) (Fig. 1). In the case of *Rv0678* Ile16fs, the insertion of 12
232 nucleotides caused the addition of 4 aa from position 16 of the Rv0678 protein without
233 disrupting the frame of the whole enzyme, while the Ala153fs caused a change to the last
234 13 aa of the C-terminal of the protein (Fig 1). This suggests that these frameshifts do not
235 affect protein stability and function resulting in the BDQ-susceptible phenotype.
236 A structural analysis of the effect of mutations in Rv0678 resulting in amino acid changes
237 was performed as previously described by the Eris and MAESTRO computational
238 approaches (Dataset S2). The Rv0678 folding stability calculation by ERIS software
239 showed that both Arg96Trp and Met111Lys mutations associated with the BDQ-resistant
240 phenotype altered Rv0678 protein folding/stability (ΔΔG kcal/mol >5). These two mutations
241 are localized in the dsDNA-binding and dimerization domain regions of Rv0678,
242 respectively (Fig. 2). Interestingly, the Met111Val mutation had a milder effect on the
243 protein stability than Met111Lys which is reflected in the low BDQ MIC value. Both Eris
244 and MAESTRO analysis showed that the other mutations in Rv0678 have a lower
245 estimated effect on protein stability which is in accordance with lower MIC values for these
246 clinical strains (Dataset S2). As these approaches do not consider the effect of the

mutations on dimerization protein function, we calculated the protein-protein binding free energy under the MM/GBSA approximation for the mutations which localize in the Rv0678 dimerization domain (Fig. 2). The results showed that five mutations (Met111Lys, Leu117Arg, Val120Met, Asp141His and Met146Arg) have a significant increase of ΔΔG kcal/mol in the protein-protein homodimer binding free energies, indicating that they can affect the dimerization process, destabilizing the overall homodimer stability (Dataset 2). This data suggest that these mutations could be directly involved in the slight increase in BDQ MIC for these strains, all with a BDQ MIC of 0.12 µg/ml except for the MTBc strain harboring the *Rv067*8 Met146Arg variant with a BDQ MIC of 0.06 µg/ml. (Fig. 2).

An analysis of correlation between observed mutations in *Rv0678*, *atpE* and *pepQ* regions with lineage and country of origin, revealed that the majority of mutations (*n*= 46; 75.4%) occurred only once (Fig. 3). Only four mutations, all in *Rv0678* gene, were detected in more than 5 isolates, all of them showing a BDQ-susceptible phenotype: the a-4t mutation in the promoter region of *Rv0678* was found in 12 Beijing (2,2,1) isolates from Azerbaijan, the Val3Ile mutation in 8 LAM (4,3,4,2) isolates from Bangladesh, Asn4Thr in 6 Delhi-CAS (3) isolates from Pakistan and Gly87Arg in 8 EAI (1,1,2) isolates from Bangladesh and Pakistan (Fig. 3).

Looking at the BDQ-resistance associated variants, the two frameshift mutations associated with high level of BDQ MICs were both observed in isolates from Pakistan and belonged to EAI (1,1,2) and Delhi-CAS (3) lineages, while the two *Rv0678* mutations associated with low level of BDQ resistance, Arg96Trp and Met111Lys, were both observed in two isolates from Bangladesh belonging to Delhi-CAS (3) and Haarlem (4,2,1,2) lineages (Fig. 3).

3.2. Analysis of mutations for DLM resistance

The 643 MTBc isolates identified by WGS as harbouring at least one mutation in one of the candidate genes for DLM resistance represented 164 unique DLM-related mutations. The WGS analysis revealed 30 unique mutations in *ddn* (including 3 nonsense and 2 frameshift mutations), 25 unique mutations in *fbiA* (including 1 nonsense mutation), 23 unique mutations in *fbiB*, 65 unique mutations in *fbiC* (including 2 frameshift mutations) and 24 unique mutations in *fgd1* gene (Dataset S1).

Considering all unique mutations, twenty (12.2%) were combinations of two or three variants in more than one candidate gene. Phenotypic results revealed that out of the 124 isolates tested for DLM, 26 (21%) were resistant to DLM, 13 (10.5%) showed a low level of resistance (MIC = 0.12 µg/ml), while 85 (68.5%) were DLM susceptible (Dataset S1). The DLM-resistant isolates spanned 32 different mutations (Table 2). Considering the phenotypic drug resistance profiles of the DLM-resistant isolates, only six were MDR-TB strains, five of which were retreatment TB cases and one was a new TB case. The analysis of mutation types associated with DLM-resistant revealed 3 nonsense mutations leading to truncated proteins, 3 frameshift mutations and 26 nonsynonymous mutations leading to a single amino acid change (Table 2).

Overall, the MIC levels among DLM-resistant isolates ranged from 0.12 µg/ml to ≥4 µg/ml, with the highest MIC values occurring with mutation types causing a truncated Ddn or FbiA protein (frameshift or stop codon mutations). The remaining mutations were associated with increased DLM MIC values between 0.12 and 0.5 µg/ml. Opposite to the high MIC level (≥4 µg/ml) observed for the frameshift at codon 14 in the *ddn* gene, the observed frameshift at the very end of the *fbiC* gene (codon 855) caused a lower increase in MIC level at 0.5 µg/ml (Table 2).

Similar to Rv0678, the mutation structural analysis was performed for the Ddn (PDB 3R5L; 3R5R) and Fgd1 (PDB 3B4Y; 3C8N) proteins (Dataset S2). The highly conserved Ddn

protein catalyzes the reduction of nitroimidazoles of DLM prodrug by the co-factor F420-H_2, resulting in intracellular release of lethal reactive nitrogen species (**36**). For the on-target Ddn protein, mutations Asn91Thr and Pro86Thr localize very close to the cofactor binding site (Fig 4A) and ΔDSX energies resulted from DrugScore analysis indicate that these are the only two mutations which reduce binding affinity between Ddn and the cofactor F420-H_2 (Dataset S2). The Ddn mutation Thr140Ile is far from the cofactor binding site but its effect on MIC increase is due to the protein folding stability, because the side chain of Thr140 residue is involved in the hydrogen bond network with Ala82-Lys79-F420-H_2 (Fig. 4A). The mutation Val61Gly, which has a mild effect on the MIC (0.12 µg/ml), showed high levels of ΔΔG Kcal/mol with both the Eris and MAESTRO analyses, suggesting a role in destabilizing the folding protein in the β-sheet (Fig. 4A). The analysis of point mutations in Ddn without available MIC values revealed a high level of ΔΔG Kcal/mol energy for mutations Arg72Gln, Pro86Thr and Glu150Ala, suggesting their potential involvement on Ddn stability and consequently phenotypic DLM resistance (Dataset S2).

The DLM off-target F420-dependent glucose-6-phosphate dehydrogenase (Fgd1) is important in MTBc energy metabolism, and it is implicated in DLM redox processes related to non-replicating persistence by providing the reduced co-factor F420-H_2 (**35**). The reported MIC values did not show a strong effect in the *in vitro* experiments because all identified mutations are further than 10 Å from the co-factor F420 binding site (Fig. 4B). Moreover, the computational Eris approach predicts that two Fgd1 mutations without phenotypic data, Ala27Gly and Val165Leu, have potential roles in protein destabilization (Dataset S2). The Fgd1 mutation Gly314Glu which was observed in a strain with only a moderate increase of DLM MIC level seemed to poorly correlate with DLM phenotype,

suggesting that other factors could contribute to this small variation of the DLM MIC level in MTBc strains.

The distribution analysis of mutations across genotypes and country of isolation showed that *ddn* mutations involved in a DLM-resistant phenotype are represented only once or twice. Exception are, Pro2Gln which was found in seven mainly-T (4,8) isolates (all from Azerbaijan), Asn91Thr in *ddn* in combination with mutation Val58Ile in *fbiA* in three mainly-T (4,8) isolates (two from Azerbaijan and one from Ukraine), and the high-level resistant stop codon mutation Gln58STOP which was detected in three Beijing (2,2,1) isolates from Ukraine (Fig. 5A). Two DLM-resistant mutations in the *fbiA-fbiB* region were seen in a single isolate, while the *fbiB* mutation Asp224Asn was found in two Delhi-CAS (3) isolates from Bangladesh. Mutation type Ile208Val in *fbiA* was the most prevalent and seen in 22 isolates, all belonging to the Euro-American lineage (Clade1; 4,1,2) and isolated in South Africa (*n*= 19), Bangladesh (*n*= 2) and Ukraine (*n*= 1) (Fig. 5B). Four of the seven DLM-resistant *fbiC* mutation types were seen in single isolates, one was observed in two isolates while two were more prevalent: the frameshift mutation Ala855fs (a deletion of 62 nt) which was detected in 30 isolates from South Africa belonging to eight different lineages, and mutation Ala835Val detected in 18 EAI (1,1,3) isolates from Bangladesh only (Fig. 6). Of note, most of the DLM-resistant strains with high-level of DLM MIC were isolated in Bangladesh (75%) and mutations were detected in *ddn* (46%), *fbiC* (31%), *fbiA* (15%) and *fbiB* (8%) (Dataset S1).

Cluster analysis by distance matrix was also performed in order to understand if the observation of three or more isolates with mutations associated with DLM resistance were potential clonal clusters. Results showed that the three Beijing (2,2,1) isolates harbouring the stop codon mutation Gln58STOP in *ddn* gene were part of the same transmission chain, at 12 SNPs cut-off (Fig. S2). Moreover, ten other clusters of two isolates each were

identified in all the other groups harbouring mutation associated with DLM resistance: four clusters of isolates with the Ile208Val mutation in *fbiA*, one cluster of isolates with Ala855fs variant in *fbiC*, two clusters of isolates with Pro2Gln in *ddn*, one cluster of isolates with Asn91Thr and Val58Ile mutations in *ddn* and *fbiA* respectively, and two clusters of isolates with *fbiC* Ala835Val (Fig. S2).

4. Discussion and Conclusion

Bedaquiline (BDQ) and delamanid (DLM) have expanded available treatment options and improved treatment success rates for patients with pulmonary MDR-TB and XDR-TB (**44, 45, 46, 47**), including children with MDR-TB (**48, 49**). The detection of resistance to BDQ and DLM is critical to ensuring effective treatment and care for DR-TB patients and preventing ongoing transmission. Although evidence for the validation and standardization of efficient methods for MICs and the setting of breakpoints for BDQ and DLM continues to expand (**22, 34, 50, 51**), there is still a notable lack of suitable data on resistance-related genomic variants (**52**). Moreover, phenotypic methods are too slow to provide early indication of susceptibility status at the time of treatment initiation. An accurate classification of SNPs according to their association with drug resistance is therefore essential to allow the use of WGS to guide the composition of treatment regimens (**7, 53**). The fact that accurate databases with catalogued mutations are currently lacking for these drugs, represent a serious limitation for molecular DST for BDQ and DLM.

To tackle this, we used a unique dataset containing 4795 WGS data of MTBc isolates from different countries with either a higher burden of TB or MDR-TB (Azerbaijan, Bangladesh, Belarus, South Africa, Pakistan and Ukraine) as a unique and accurate source of genetic information for the characterization and validation of genomic variants potentially involved in BDQ and DLM resistance. In particular, this study highlighted the role of genetic variants for BDQ and DLM resistance development by combining the MICs results of MTBc isolates

with variants and the *in silico* analysis on available protein structures, paving the way for the construction of an encyclopaedia of characterized mutations to be use for molecular DST.

From the whole WGS dataset, we identified 61 different BDQ-related variants in *Rv0678*, *atpE* promoter and *pepQ* genomic regions, out of which four were associated to BDQ-resistant phenotype: two frameshift mutations in Rv0678 associated to a high levels of BDQ MIC and two non-synonymous mutations found associated to low levels of BDQ resistance. To the best of our knowledge, among these four BDQ-resistant mutations, only the frameshift mutation Gly6fs (del_16-17 gg) has been previously described in one BDQ-resistant isolate (**54**). In agreement with the *in vitro* MIC experiments, the *in silico* structural analysis on the Rv0678 single monomer protein form (PDB 4N5B) showed that mutations Met111Lys and Arg96Trp have very high Eris and MAESTRO ΔΔG Kcal/mol energy values, indicating a strong destabilization of the protein folding. The mutations Gly87Arg and Leu117Arg in *Rv0678* were previously described in BDQ-susceptible strains (**13**), confirming the detected low MIC of 0.03 µg/ml and 0.12 µg/ml, respectively. (Dataset S1). The role of Leu117Arg remains unclear as another study described this mutation as associated with both BDQ and also CLF resistance (**11**). However, our phenotypic and *in silico* results suggest that Leu117Arg affects the dimerization of Rv0678 causing a small increase but not high-level value of BDQ MIC. Other mutations in *Rv0678* were described at the same codon position but with a different amino acid change (**5, 8, 9, 11, 13**). The *Rv0678* mutations Val20Phe, Ala84Glu and Arg90Pro were observed to be linked to increase MICs for CLF and potentially associated to a BDQ-resistant phenotype, while Val20Gly was associated with both BDQ and CLF resistance (**5, 9**). In this study, *Rv0678* mutations Val20Ala and Ala84Val were found in BDQ-susceptible strains (MIC ≤ 0.008 µg/ml), while Arg90Cys was associated with a BDQ MIC value of 0.12 µg/ml. Moreover, *in*

silico analysis confirmed that the Arg90Cys mutation can have a mild effect on protein stability and a role in the small variation of BDQ MIC. Mutations Arg96Gln, Met146Thr and Leu136Pro *in Rv0678* have been described with increased MIC values for BDQ (**8, 11, 13**). In our dataset, strains harbouring mutations at the same codons were not consistently phenotypically resistant, with mutations Arg96Trp, Met146Arg and Leu136Val respectively showing MICs of 0.25 µg/ml (BDQ-resistant), 0.06 µg/ml (BDQ-susceptible) and 0.03 µg/ml (BDQ-susceptible). Again, *in silico* analysis results were in agreement with the phenotypic data, showing that only the Arg96Trp mutation highly destabilized Rv0678 folding while the other two mutations showed a lower ΔΔG Kcal/mol energy values (Dataset S2). Furthermore, the *in silico* MM/GBSA analysis, revealed that Rv0678 mutations Leu117Arg, Val120Met and Asp141His can affect the protein homodimerization, which could explain the slight increase of BDQ MIC to 0.12 µg/ml for these MTBc strains, yet still classified as BDQ-susceptible despite being close to the proposed cut-off.

Considering the five genomic regions associated with DLM phenotype (*ddn*, *fgd1*, *fbiA*, *fbiB* and *fbiC*), the WGS analysis revealed a total of 164 unique mutations potentially involved in DLM resistance. Apart from seven previously characterized mutations (**16**), all the other 156 DLM-related variants have not been previously described earlier except for Asn91Thr in *ddn*, for which we confirmed its role in DLM resistance (**18**). Phenotypic results on a subset of available isolates showed that 32 different mutations, detected in all of the considered genomic regions were associated to DLM resistance. Notably, the *in silico* mutation structural analysis revealed that the effect of the point mutations in Ddn and Fgd1 were in agreement with the MIC results (Dataset S2). Indeed, the mutation Asn91Thr in Ddn is directly involved in the binding with the co-factor F420-H_2 by disrupting the Ddn-F420-H_2 interaction but also in destabilizing the Ddn folding and mutations Val61Gly and Thr140Ile, which were observed in MTBc strains with MICs for DLM of 0.12 µg/ml and 0.5

µg/ml respectively, showed also a potential effect on Ddn protein folding and stability. Furthermore, the *in silico* analysis indicates that three mutations in Ddn for which corresponding phenotypic data were not available (Arg72Gln, Pro86Thr, Glu150Ala) may have a significant impact on protein stability and thereby play a role in the DLM-resistant phenotype.

In addition, the correlation analysis between mutations linked to BDQ- and DLM-resistant phenotypes and metadata information corroborate with previously reported data, suggesting the absence of links between BDQ or DLM resistance and strain lineage or drug resistance profiles of MTBc isolates (**10, 16**). Globally, considering DST profiles of BDQ- and DLM-resistant strains, 75% were fully susceptible, 6% were MDR-TB, and the majority of them (68.7%) was from new TB cases. Moreover, the analysis of country-lineage distribution did not reveal any significant correlation between BDQ/DLM-related mutations and lineage groups or country of isolation. To complete this set of analyses, we also performed a SNP-based distance matrix to evaluate the relatedness of strains harbouring the most frequent DLM-resistant variants, showing that for these groups there are no major transmission chains but only small clusters of two to three isolates, meaning that these resistance-associated mutations can rise spontaneously and independently. Conversely, none of the BDQ-resistant variants were detected in isolates groups.

In conclusion, our study provides novel and important evidence on the role of mutations associated with BDQ- and DLM-resistant phenotypes. A concerningly high prevalence of genetic mutations associated with an increased MIC was detected in clinical isolates from patients who have never been exposed to these drugs, supporting previous findings (**10, 16**). Also, our data showed that different non-synonymous or indel mutation at the same nucleotide position can display a completely different phenotypic effect or different level of resistance, thus reinforcing the need to accurately investigate the role of each individual

mutation. Equally important, these findings also showed the presence of 125 genetic variants not associated with BDQ and DLM resistance, scattered over the full length of each target gene. Therefore, considering the complexity of BDQ and DLM mechanisms of resistance and the absence of fully standardized phenotypic tests, the development of accurate molecular-based DST is wholly dependent on the establishment of a complete database of validated mutations, a scenario which is comparable to the challenges associated with molecular markers of resistance to pyrazinamide (PZA) (**55**). The establishment of a common database combining data from MTBc isolates collected in a large number of settings with the inclusion of different parameters (phenotype, genotype, structure, and free energy analyses) is fundamental to improve our understanding of the role of mutations in determining the BDQ/DLM susceptibility phenotype. Finally, this database could be also beneficial to study genetic resistance to other drugs that could be potentially sharing similar genetic basis of resistance such as clofazimine for BDQ and pretomanid for DLM.

For these reasons, despite some limitations (not all strains were available for MIC determination, absence of standardized methods and breakpoints for the interpretation of BDQ and DLM phenotypes, absence of 3D structures of FbiA, FbiB, FbiC and PepQ proteins for *in silico* investigation, lack of knowledge of other genomic regions potentially involved in BDQ/DLM resistance), this work will be an important source of information for new genome-based sequencing approaches for predicting BDQ and DLM resistance.

References

1. World Health Organization. 2019. Global Tuberculosis Report, 2019. WHO, Geneva. https://www.who.int/tb/publications/global_report/en/
2. World Health Organization. 2019. Consolidated guidelines on drug-resistant tuberculosis treatment. WHO, Geneva.

https://www.who.int/tb/publications/2019/consolidated-guidelines-drug-resistant-TB-treatment/en/

3. Bloemberg GV, Keller PM, Stucki D, Trauner A, Borrell S, Latshang T, Coscolla M, Rothe T, Hömke R, Ritter C, Feldmann J, Schulthess B, Gagneux S, Böttger EC. 2015. Acquired Resistance to Bedaquiline and Delamanid in Therapy for Tuberculosis. *N Engl J Med* **12**:1986-1988. doi: 10.1056/NEJMc1505196
4. Hoffmann H, Kohl T, Hofmann-Thiel S, Merker M, Beckert P, Jaton K, Nedialkova L, Sahalchyk E, Rothe T, Keller PM, Niemann S. 2016. Delamanid and Bedaquiline Resistance in *Mycobacterium tuberculosis* Ancestral Beijing Genotype Causing Extensively Drug-Resistant Tuberculosis in a Tibetan Refugee. *Am J Respir Crit Care Med* **193**:337-340. doi: 10.1164/rccm.201502-0372LE
5. Ghodousi A, Rizvi AH, Baloch AQ, Ghafoor A, Khanzada FM, Qadir M, Borroni E, Trovato A, Tahseen S, Cirillo DM. 2019. Acquisition of Cross-Resistance to Bedaquiline and Clofazimine following Treatment for Tuberculosis in Pakistan. *Antimicrob Agents Chemother* **63**:e00915-19. doi: 10.1128/AAC.00915-19
6. Polsfuss S, Hofmann-Thiel S, Merker M, Krieger D, Niemann S, Rüssmann H, Schönfeld N, Hoffmann H, Kranzer K. 2019. Emergence of Low-level Delamanid and Bedaquiline Resistance During Extremely Drug-resistant Tuberculosis Treatment. *Clin Infect Dis* **69**:1229-1231. doi: 10.1093/cid/ciz074
7. Andres S, Merker M, Heyckendorf J, Kalsdorf B, Rumetshofer R, Indra A, Hofmann-Thiel S, Hoffmann H, Lange C, Niemann S, Maurer FP. 2020. Bedaquiline-resistant Tuberculosis: Dark Clouds on the Horizon. *Am J Respir Crit Care Med* Online ahead of print. doi: 10.1164/rccm.201909-1819LE
8. Torrea G, Coeck N, Desmaretz C, Van De Parre T, Van Poucke T, Lounis N, de Jong BC, Rigouts L. 2015. Bedaquiline susceptibility testing of *Mycobacterium*

tuberculosis in an automated liquid culture system. *J Antimicrob Chemother* **70**:2300-2305. doi: 10.1093/jac/dkv117

9. Zhang S, Chen J, Cui P, Shi W, Zhang W, Zhang Y. 2015. Identification of novel mutations associated with clofazimine resistance in *Mycobacterium tuberculosis*. *J Antimicrob Chemother* **70:**2507-2510. doi: 10.1093/jac/dkv150
10. Villellas C, Coeck N, Meehan CJ, Lounis N, de Jong B, Rigouts L, Andries K. 2017. Unexpected high prevalence of resistance-associated Rv0678 variants in MDR-TB patients without documented prior use of clofazimine or bedaquiline. *J Antimicrob Chemother* **72**:684-690. doi: 10.1093/jac/dkw502
11. Xu J, Wang B, Hu M, Huo F, Guo S, Jing W, Nuermberger E, Lu Y. 2017. Primary Clofazimine and Bedaquiline Resistance among Isolates from Patients with Multidrug-Resistant Tuberculosis. *Antimicrob Agents Chemother* **61**:e00239-17. doi: 10.1128/AAC.00239-17
12. Ismail NA, Omar SV, Joseph L, Govender N, Blows L, Ismail F, Koornhof H, Dreyer AW, Kaniga K, Ndjeka N. 2018. Defining Bedaquiline Susceptibility, Resistance, Cross-Resistance and Associated Genetic Determinants: A Retrospective Cohort Study. *EBioMedicine* **28**:136-142. doi: 10.1016/j.ebiom.2018.01.005
13. Martinez E, Hennessy D, Jelfs P, Crighton T, Chen SC, Sintchenko V. 2018. Mutations associated with in vitro resistance to bedaquiline in *Mycobacterium tuberculosis* isolates in Australia. *Tuberculosis (Edinb)* **111**:31-34. doi: 10.1016/j.tube.2018.04.007
14. Kardan-Yamchi J, Kazemian H, Battaglia S, Abtahi H, Foroushani AR, Hamzelou G, Cirillo DM, Ghodousi A, Feizabadi MM. 2020. Whole Genome Sequencing Results Associated with Minimum Inhibitory Concentrations of 14 Anti-Tuberculosis Drugs

among Rifampicin-Resistant Isolates of *Mycobacterium tuberculosis* from Iran. *J Clin Med* **9**:E465. doi: 10.3390/jcm9020465

15. Feuerriegel S, Köser CU, Baù D, Rüsch-Gerdes S, Summers DK, Archer JA, Marti-Renom MA, Niemann S. 2011. Impact of Fgd1 and ddn diversity in *Mycobacterium tuberculosis* complex on in vitro susceptibility to PA-824. *Antimicrob Agents Chemother* **55**:5718–5722. doi: 10.1128/AAC.05500-11
16. Schena E, Nedialkova L, Borroni E, Battaglia S, Cabibbe AM, Niemann S, Utpatel C, Merker M, Trovato A, Hofmann-Thiel S, Hoffmann H, Cirillo DM. 2016. Delamanid susceptibility testing of *Mycobacterium tuberculosis* using the resazurin microtitre assay and the BACTEC™ MGIT™ 960 system. *J Antimicrob Chemother* **71**:1532-1539. doi: 10.1093/jac/dkw044
17. Pang Y, Zong Z, Huo F, Jing W, Ma Y, Dong L, Li Y, Zhao L, Fu Y, Huang H. 2017. In Vitro Drug Susceptibility of Bedaquiline, Delamanid, Linezolid, Clofazimine, Moxifloxacin, and Gatifloxacin against Extensively Drug-Resistant Tuberculosis in Beijing, China. *Antimicrob Agents Chemother* **61**:e00900-17. doi: 10.1128/AAC.00900-17
18. Fujiwara M, Kawasaki M, Hariguchi N, Liu Y, Matsumoto M. 2018. Mechanisms of resistance to delamanid, a drug for *Mycobacterium tuberculosis*. *Tuberculosis (Edinb)* **108**:186-194. doi: 10.1016/j.tube.2017.12.006
19. Yang JS, Kim KJ, Choi H, Lee SH. 2018. Delamanid, Bedaquiline and Linezolid Minimum Inhibitory Concentration Distributions and Resistance-related Gene Mutations in Multidrug-resistant and Extensively Drug-resistant Tuberculosis in Korea. *Ann Lab Med* **38**:563-568. doi: 10.3343/alm.2018.38.6.563
20. Wen S, Jing W, Zhang T, Zong Z, Xue Y, Shang Y, Wang F, Huang H, Chu N, Pang Y. 2019. Comparison of in vitro activity of the nitroimidazoles delamanid and

544 pretomanid against multidrug-resistant and extensively drug-resistant tuberculosis.
545 *Eur J Clin Microbiol Infect Dis* **38**:1293-1296. doi: 10.1007/s10096-019-03551-w
546 21. Ellington MJ, Ekelund O, Aarestrup FM, Canton R, Doumith M, Giske C, Grundman
547 H, Hasman H, Holden MTG, Hopkins KL, Iredell J, Kahlmeter G, Köser CU,
548 MacGowan A, Mevius D, Mulvey M, Naas T, Peto T, Rolain JM, Samuelsen Ø,
549 Woodford N. 2017. The role of whole genome sequencing in antimicrobial
550 susceptibility testing of bacteria: report from the EUCAST Subcommittee. *Clin*
551 *Microbiol Infect* **23**:2–22. 10.1016/j.cmi.2016.11.012
552 22. Meehan CJ, Goig GA, Kohl TA, Verboven L, Dippenaar A, Ezewudo M, Farhat MR,
553 Guthrie JL, Laukens K, Miotto P, Ofori-Anyinam B, Dreyer V, Supply P, Suresh A,
554 Utpatel C, van Soolingen D, Zhou Y, Ashton PM, Brites D, Cabibbe AM, de Jong
555 BC, de Vos M, Menardo F, Gagneux S, Gao Q, Heupink TH, Liu Q, Loiseau C,
556 Rigouts L, Rodwell TC, Tagliani E, Walker TM, Warren RM, Zhao Y, Zignol M,
557 Schito M, Gardy J, Cirillo DM, Niemann S, Comas I, Van Rie A. 2019. Whole
558 genome sequencing of *Mycobacterium tuberculosis*: current standards and open
559 issues. *Nat Rev Microbiol* **17**:533-545. doi: 10.1038/s41579-019-0214-5
560 23. Andries K, Verhasselt P, Guillemont J, Göhlmann HW, Neefs JM, Winkler H, Van
561 Gestel J, Timmerman P, Zhu M, Lee E, Williams P, de Chaffoy D, Huitric E, Hoffner
562 S, Cambau E, Truffot-Pernot C, Lounis N, Jarlier V. 2005. A diarylquinoline drug
563 active on the ATP synthase of *Mycobacterium tuberculosis*. *Science* **307**:223-227.
564 doi: 10.1126/science.1106753
565 24. Andries K, Villellas C, Coeck N, Thys K, Gevers T, Vranckx L, Lounis N, de Jong
566 BC, Koul A. 2014. Acquired resistance of *Mycobacterium tuberculosis* to
567 bedaquiline. *PLoS One* **9**:e102135. doi: 10.1371/journal.pone.0102135

568 25. Almeida D, Ioerger T, Tyagi S, Li SY, Mdluli K, Andries K, Grosset J, Sacchettini J,
569 Nuermberger E. 2016. Mutations in pepQ Confer Low-level Resistance to
570 Bedaquiline and Clofazimine in *Mycobacterium tuberculosis*. *Antimicrob Agents*
571 *Chemother* **60**:4590-4599. doi: 10.1128/AAC.00753-16
572 26. Haver HL, Chua A, Ghode P, Lakshminarayana SB, Singhal A, Mathema B,
573 Wintjens R, Bifani P. 2015. Mutations in genes for the F420 biosynthetic pathway
574 and a nitroreductase enzyme are the primary resistance determinants in
575 spontaneous in vitro-selected PA-824-resistant mutants of *Mycobacterium*
576 *tuberculosis*. *Antimicrob Agents Chemother* **59**:5316-5323. doi:
577 10.1128/AAC.00308-15
578 27. Matsumoto M, Hashizume H, Tomishige T, Kawasaki M, Tsubouchi H, Sasaki H,
579 Shimokawa Y, Komatsu M. 2006. OPC-67683, a nitrodihydro-imidazooxazole
580 derivative with promising action against tuberculosis in vitro and in mice. *PLoS Med*
581 **3**:e466 doi: 10.1371/journal.pmed.0030466
582 28. Zignol M, Cabibbe AM, Dean AS, Glaziou P, Alikhanova N, Ama C, Andres S,
583 Barbova A, Borbe-Reyes A, Chin DP, Cirillo DM, Colvin C, Dadu A, Dreyer A,
584 Driesen M, Gilpin C, Hasan R, Hasan Z, Hoffner S, Hussain A, Ismail N, Kamal
585 SMM, Khanzada FM, Kimerling M, Kohl TA, Mansjö M, Miotto P, Mukadi YD, Mvusi
586 L, Niemann S, Omar SV, Rigouts L, Schito M, Sela I, Seyfaddinova M, Skenders G,
587 Skrahina A, Tahseen S, Wells WA, Zhurilo A, Weyer K, Floyd K, Raviglione MC.
588 2018. Genetic sequencing for surveillance of drug resistance in tuberculosis in
589 highly endemic countries: a multi-country population-based surveillance study.
590 *Lancet Infect Dis* **18**:675-683. doi: 10.1016/S1473-3099(18)30073-2
591 29. Kohl TA, Utpatel C, Schleusener V, De Filippo MR, Beckert P, Cirillo DM, Niemann
592 S. 2018. MTBseq: a comprehensive pipeline for whole genome sequence analysis

593 of *Mycobacterium tuberculosis* complex isolates. *PeerJ* **6**:e5895. doi:
594 10.7717/peerj.5895

595 30. Lew JM, Kapopoulou A, Jones LM, Cole ST. 2011. TubercuList--10 years
596 after. *Tuberculosis (Edinb)* **91**:1-7. doi: 10.1016/j.tube.2010.09.008

597 31. Meehan CJ, Moris P, Kohl TA, Pečerska J, Akter S, Merker M, Utpatel C, Beckert
598 P, Gehre F, Lempens P, Stadler T, Kaswa MK, Kühnert D, Niemann S, de Jong BC.
599 2018. The relationship between transmission time and clustering methods in
600 *Mycobacterium tuberculosis* epidemiology. *EBioMedicine* **37**:410-416.
601 doi: 10.1016/j.ebiom.2018.10.013

602 32. Lopez B, Siqueira de Oliveira R, Pinhata JMW, Chimara E, Pacheco Ascencio E,
603 Puyén Guerra ZM, Wainmayer I, Simboli N, Del Granado M, Palomino JC, Ritacco
604 V, Martin A. 2019. Bedaquiline and linezolid MIC distributions and epidemiological
605 cut-off values for *Mycobacterium tuberculosis* in the Latin American region. *J*
606 *Antimicrob Chemother* **74**:373-379. doi: 10.1093/jac/dky414

607 33. Palomino JC, Martin A, Camacho M, Guerra H, Swings J, Portaels F. 2002.
608 Resazurin microtiter assay plate: simple and inexpensive method for detection of
609 drug resistance in *Mycobacterium tuberculosis*. *Antimicrob Agents Chemother*
610 **46**:2720-2722. doi: 10.1128/aac.46.8.2720-2722.2002

611 34. World Health Organization. 2018. Technical Report on critical concentrations for
612 drug susceptibility testing of medicines used in the treatment of drug-resistant
613 tuberculosis. WHO, Geneva. WHO/CDS/TB/2018.5

614 35. Bashiri G, Squire CJ, Moreland NJ, Baker EN. 2008. Crystal structures of F420-
615 dependent glucose-6-phosphate dehydrogenase FGD1 involved in the activation of
616 the anti-tuberculosis drug candidate PA-824 reveal the basis of coenzyme and
617 substrate binding. *J Biol Chem* **283**:17531-17541. doi: 10.1074/jbc.M801854200

618 36. Cellitti SE, Shaffer J, Jones DH, Mukherjee T, Gurumurthy M, Bursulaya B, Boshoff
619 HI, Choi I, Nayyar A, Lee YS, Cherian J, Niyomrattanakit P, Dick T, Manjunatha UH,
620 Barry CE 3rd, Spraggon G, Geierstanger BH. 2012. Structure of Ddn, the
621 deazaflavin-dependent nitroreductase from *Mycobacterium tuberculosis* involved in
622 bioreductive activation of PA-824. *Structure* **20**:101-112. doi:
623 10.1016/j.str.2011.11.001
624 37. Radhakrishnan A, Kumar N, Wright CC, Chou TH, Tringides ML, Bolla JR, Lei HT,
625 Rajashankar KR, Su CC, Purdy GE, Yu EW. 2014. Crystal structure of the
626 transcriptional regulator Rv0678 of *Mycobacterium tuberculosis. J Biol Chem*
627 **289**:16526-16540. doi: https://doi.org/10.1074/jbc.M113.538959
628 38. Yin S, Ding F, Dokholyan NV. 2007 Eris: an automated estimator of protein stability.
629 *Nat Methods* **4**:466-467. doi: 10.1038/nmeth0607-466
630 39. Laimer J, Hofer H, Fritz M, Wegenkittl S, Lackner P. 2015. MAESTRO - multi agent
631 stability prediction upon point mutations. *BMC Bioinformatics* **16**:116.
632 doi: 10.1186/s12859-015-0548-6
633 40. Neudert G, Klebe G. 2011. DSX: a knowledge-based scoring function for the
634 assessment of protein-ligand complexes. *J Chem Inf Model* **51**:2731-2745. doi:
635 10.1021/ci200274q
636 41. Miller BR 3rd, McGee TD Jr, Swails JM, Homeyer N, Gohlke H, Roitberg AE. 2012
637 MMPBSA.py: An Efficient Program for End-State Free Energy Calculations. *J Chem*
638 *Theory Comput* **8**:3314–3321. doi: 10.1021/ct300418h
639 42. Larkin MA, Blackshields G, Brown NP, Chenna R, McGettigan PA, McWilliam H,
640 Valentin F, Wallace IM, Wilm A, Lopez R, Thompson JD, Gibson TJ, Higgins DG.
641 2007. Clustal W and Clustal X version 2.0. *Bioinformatics* **23**:2947–2948.
642 doi: 10.1093/bioinformatics/btm404

643 43. The PyMOL Molecular Graphics System, Version 2.0 Schrödinger, LLC.
644 44. Migliori GB, Pontali E, Sotgiu G, Centis R, D'Ambrosio L, Tiberi S, Tadolini M,
645 Esposito S. 2017. Combined Use of Delamanid and Bedaquiline to Treat Multidrug-
646 Resistant and Extensively Drug-Resistant Tuberculosis: A Systematic Review. *Int J*
647 *Mol Sci* **18**:341. doi: 10.3390/ijms18020341
648 45. Ferlazzo G, Mohr E, Laxmeshwar C, Hewison C, Hughes J, Jonckheere S,
649 Khachatryan N, De Avezedo V, Egazaryan L, Shroufi A, Kalon S, Cox H, Furin J,
650 Isaakidis P. 2018. Early safety and efficacy of the combination of bedaquiline and
651 delamanid for the treatment of patients with drug-resistant tuberculosis in Armenia,
652 India, and South Africa: a retrospective cohort study. *Lancet Infect Dis* **18**:536–544.
653 doi: 10.1016/S1473-3099(18)30100-2
654 46. Li Y, Sun F, Zhang W. 2019. Bedaquiline and delamanid in the treatment of
655 multidrug-resistant tuberculosis: Promising but challenging. *Drug Dev Res* **80**:98-
656 105. doi: 10.1002/ddr.21498
657 47. Olayanju O, Esmail A, Limberis J, Dheda K. 2020. A regimen containing
658 bedaquiline and delamanid compared to bedaquiline in patients with drug-resistant
659 tuberculosis. *Eur Respir J* **55**:1901181. doi: 10.1183/13993003.01181-2019
660 48. World Health Organization. 2016. The Use of Delamanid in the Treatment of
661 Multidrug-Resistant Tuberculosis in Children and Adolescents: Interim Policy
662 Guidance. WHO, Geneva. WHO/HTM/TB/2016.14
663 49. Achar J, Hewison C, Cavalheiro AP, Skrahina A, Cajazeiro J, Nargiza P, Herboczek
664 K, Rajabov AS, Hughes J, Ferlazzo G, Seddon JA, du Cros P. 2017. Off-Label Use
665 of Bedaquiline in Children and Adolescents with Multidrug-Resistant Tuberculosis.
666 *Emerg Infect Dis* **23**:1711–1713. doi: DOI: 10.3201/eid2310.170303

50. Rancoita PMV, Cugnata F, Gibertoni Cruz AL, Borroni E, Hoosdally SJ, Walker TM, Grazian C, Davies TJ, Peto TEA, Crook DW, Fowler PW, Cirillo DM, CRyPTIC Consortium. 2018. Validating a 14-Drug Microtiter Plate Containing Bedaquiline and Delamanid for Large-Scale Research Susceptibility Testing of *Mycobacterium tuberculosis*. *Antimicrob Agents Chemother* **62**:e00344-18. doi: 0.1128/AAC.00344-18

51. Kaniga K, Aono A, Borroni E, Cirillo DM, Desmaretz C, Hasan R, Joseph L, Mitarai S, Shakoor S, Torrea G, Ismail NA, Omar SV. 2020. Validation of Bedaquiline Phenotypic Drug Susceptibility Testing Methods and Breakpoints: a Multilaboratory, Multicountry Study. *J Clin Microbiol* **58**:e01677-19. doi: 10.1128/JCM.01677-19

52. Köser CU, Maurer FP, Kranzer K. 2019. 'Those who cannot remember the past are condemned to repeat it': Drug-susceptibility testing for bedaquiline and delamanid. *Int J Infect Dis* **80**:32-35. doi: 0.1016/j.ijid.2019.02.027

53. Cabibbe AM, Walker TM, Niemann S, Cirillo DM. 2018 Whole genome sequencing of *Mycobacterium tuberculosis*. *Eur Respir J* **52**:1801163. doi: 10.1183/13993003.01163-2018

54. Veziris N, Bernard C, Guglielmetti L, Le Du D, Marigot-Outtandy D, Jaspard M, Caumes E, Lerat I, Rioux C, Yazdanpanah Y, Tiotiu A, Lemaitre N, Brossier F, Jarlier V, Robert J, Sougakoff W, Aubry A; CNR MyRMA and the Tuberculosis Consilium of the CNR MyRMA; CNR MyRMA and Tuberculosis Consilium of the CNR MyRMA. 2017. Rapid emergence of *Mycobacterium tuberculosis* bedaquiline resistance: lessons to avoid repeating past errors. *Eur Respir J* **49**:1601719. doi: 10.1183/13993003.01719-2016

55. Miotto P, Cabibbe AM, Feuerriegel S, Casali N, Drobniewski F, Rodionova Y, Bakonyte D, Stakenas P, Pimkina E, Augustynowicz-Kopeć E, Degano M, Ambrosi

692 A, Hoffner S, Mansjö M, Werngren J, Rüsch-Gerdes S, Niemann S, Cirillo DM.
693 2014. *Mycobacterium tuberculosis* pyrazinamide resistance determinants: a
694 multicenter study. *mBio* **5**:e01819-14. doi: 10.1128/mBio.01819-14

695 **Legends**

696 **Table 1. List of *Rv0678* mutations detected in MTBc strains resistant to BDQ**. In the
697 table are reported all the information for each BDQ-resistant related mutations (MIC ≥ 0.25
698 µg/ml) and for the MTBc isolate tested for BDQ susceptibility. [a] Genomic position in
699 reference H37Rv NC_000962.3 strain; [b] Amino acid (aa) change and nucleotide (nt)
700 change; [c] Minimum Inhibitory concentration (MIC) value in µg/ml. [d] Country of MTBc
701 isolate origin: Pakistan (PAK), Bangladesh (BGD). [e] TB patient treatment history: new TB
702 case "New", or patient with previous TB history and treatment "Retreatment". [f] Drug
703 resistance pattern of the isolates: MDR (multi drug resistant strain), FQs
704 (fluoroquinolones), INH (Isoniazid), RIF (Rifampicin), R/S (resistant/susceptible).

705 **Fig. 1. Amino acid sequence alignment of BDQ-susceptible frameshift mutations in**
706 ***Rv0678***. The amino acid (aa) sequence of the translated proteins with Ile16fs and
707 Ala153fs frameshift mutations (associated to BDQ-susceptible MIC) were aligned with
708 Rv0678 wild type aa sequence using ClustalX. In both cases the two insertions mutations
709 cause the addition of new aa residues without altering the frame of Rv0678 protein and
710 functional residues of the protein.

711 **Fig. 2. Cartoon representation of Rv0678 protein structures with mutations**
712 **associated to BDQ-resistant and to BDQ-susceptible phenotypes.** Carton
713 representation of the monomer present in the X-Ray unit cell (4NB5). Highlighted in sticks
714 are reported the mutations associated to BDQ resistance (red) and susceptible (green)
715 from BDQ MIC assay. *In silico* predicted mutations which could alter dimerization or DNA
716 binding function, and predicted associated to BDQ-susceptible phenotype are shown in

717 orange and in blue respectively. Cartoon zoomed representations of Rv0678 dimerization
718 domain and DNA binding domain are reported.

719 **Fig. 3. Lineage and country distributions of MTBc strains with variants in *Rv0678*,**
720 ***atpE* and *pepQ* genomic regions.** The graph reports all mutations found in *Rv0678, atpE*
721 and *pepQ* genomic regions showing their distribution among lineages and country of
722 isolation. The histograms refer to the number of strains in which mutations were observed
723 (Y axis). The colors of the histograms represent the different countries of isolation while
724 the patterns inside each bar represent the different lineages. On the X axis, the results of
725 the MIC test for available MTBc strains are also reported: red triangle are BDQ-resistant
726 strains (MIC > 0.25 µg/ml); yellow box, are BDQ low resistance level strains, (MIC = 0.25
727 µg/ml); green triangles are BDQ-susceptible strains (MIC ≤ 0.12 µg/ml).

728 **Table 2**. **List of *ddn*, *fgd1*, *fbiA*, *fbiB* and *fbiC* mutations detected in MTBc strains**
729 **resistant to DLM**. In the table are reported all the information for each DLM-resistant
730 related mutations (MIC ≥ 0.12) and for the MTBc isolates tested for DLM susceptibility. [a]
731 Genomic position in reference H37Rv NC_000962.3 strain. [b] Amino acid change and
732 nucleotide (nt) change; [c] minimum Inhibitory concentration (MIC) value in µg/ml. [d] Country
733 of MTBc isolate origin: Pakistan (PAK), Bangladesh (BGD), Ukraine (UKR), Azerbaijan
734 (AZE), South Africa (SA). [e] Patient treatment history; new TB case “New”, or patient with
735 previous TB history and treatment “Retreatment”. [f] Drug resistance pattern of the isolates:
736 MDR (multi drug resistant strain), FQs (fluoroquinolones), INH (Isoniazid), RIF
737 (Rifampicin), R/S (resistant/susceptible).

738 **Fig. 4**. **Cartoon representation Ddn and Fgd1 protein structures with mutations**
739 **found associated to DLM-resistant or associated to DLM-susceptible phenotype. A**:
740 Ddn protein bound to F420 cofactor (3R5R) with highlighted in sticks the resistant (red),
741 susceptible (green), *in silico* DLM-resistant associated mutations (orange) and *in silico*

predicted DLM-susceptible mutations (blue). F420 is shown in magenta licorice. A zoom cartoon representation of Ddn bound to F420 is reported. The hydrogen bond network Thr140-Ala82-Lys79-F420-H2 is shown in dashed yellow line and the Ala82 and Lys79 residues are shown in sticks. **B**: Fgd1 carton representation of holo- and homodimer-Fgd1 bound to F420 (3B4Y). Helixes involved in protein dimerization are colored in cyan. Highlighted in sticks the DLM-resistant (red), DLM-susceptible (green), *in silico* predicted DLM-resistant mutations (orange) and *in silico* predicted DLM-susceptible mutations (blue).

Fig. 5. Lineage and country distributions of MTBc strains with variants in *ddn* and *fgd1* genomic regions and *fbiA-fbiB* operon region. The graph reports all mutations found in *ddn*, *fgd1* (**A**) and *fbiA, fbiB* (**B**) genomic regions, showing their distribution among lineages and country of isolation. The histograms refer to the number of strains in which mutations were observed (Y axis). The colors of the histograms represent the different countries of isolation while the patterns inside each bar represent the different lineages. On the X axis, the results of the MIC test for available MTBc strains are also reported: red triangle are DLM-resistant strains (MIC ≥ 0.12 µg/ml); yellow box are low resistance level (MIC = 0.12 µg/ml) and green triangles are DLM-susceptible strains (MIC < 0.12 µg/ml). If a mutation was previously described in literature it was also reported ("S" for strain susceptible to DLM or "R" for strain resistant to DLM).

Fig. 6. **Lineage and country distributions of MTBc strains with variants in *fbiC* genomic region**. In this graph are report all mutations found in *fbiC* genomic region showing their distribution among lineages and countries of isolation. See Fig. 5 legend for details.

Table S1. ***M. tuberculosis*** **genomic regions considered for bedaquiline and delamanid resistances**.

[a] For promoter regions, it was considered the upstream region up to the -100 position before the first nucleotide of each gene.

[b] The genomic positions are based on the reference genome of *M. tuberculosis* H37Rv NC_000962.3.

Fig. S1. Study design, number of selected *M. tuberculosis* (MTBc) isolates and DST profile categorization. **A**: phenotypic drug susceptibility test (pDST) of the whole collection which classified MTBc isolates in not-MDR, MDR and XDR strains. **B**: Flow chart scheme of isolates selection and stratifications. The blue scheme refers to MTBc isolates selected for DLM-related mutations while the red once to MTBc isolates selected for BDQ-related mutations. [a] The WHO approved study list includes 4795 whole genome sequencing (WGS) samples (accession number SRP128089). [b] Stratification by the phenotypic resistance profile for the selected isolates. Abbreviations: **not-MDR**, fully susceptible strains (full-S), mono resistant to rifampicin (RIF) or to isoniazid (INH); **MDR**, multidrug resistant strains, resistant almost to INH and RIF; **INH-R**, resistant to isoniazid; **RIF-R**, resistant to rifampicin; **FQ-R**, resistant to fluoroquinolones; **Fully-S**: susceptible to INH and RIF; **Pre-XDR**, MDR resistant also to FQ or second line injectables; **XDR**, MDR plus resistance to FQs and second-line injectables.

Dataset S1. **Samples general database.**

General database with all information of selected MTBc strains harbouring at least one mutation pattern in candidate genes for BDQ and DLM resistance. The excel database is divided in two sheets named “mutations list for BDQ” and “mutations list for DLM”. [a] WGS analysis (genomic regions for BDQ/DLM resistance) in which are report the list of mutations from WGS analysis with information of genomic locus, gene ID, genomic coordinate (reference strain H37Rv NC_000962.3), amino acid substitution and type of mutation. [b] MIC value results (µg/mL) from REMA assay (DLM/BDQ) of selected isolates

(for several mutations two different isolates were tested); empty cell means that the strain with that specific mutation was not available. [c] Previously reported mutations: If a mutation was previously reported it is indicated if linked or not to resistance phenotype. [e] Information on selected samples (isolates 1 and 2): WGS sample name in the WHO database, country of origin, lineage (coll. lineage) and DST profile of MTBc isolates selected for MIC test. [d] Lineage/Country mutation frequency distribution: numbers of MTBc isolates carrying mutations among countries of origin and strain lineage.

Dataset S2. Mutation structural analysis.

General database with all results from the *in silico* analysis of point mutations for the available crystal structures of proteins: Ddn (PDB 3R5R), Fgd1 (PDB 3B4Y) and Rv0678 (PDB 4NB5). Free energy calculation (ΔΔG kcal/mol) of all amino acid change mutations were performed with Eris, an automated estimator of protein stability and MAESTRO, an approach for multi agent stability prediction upon point mutations. DrugScore (DSX) software, a Knowledge-Based Scoring Function for the Assessment of Protein–Ligand Complexes, was used for Ddn-F420 and Fgd1-F420 complexes analysis. The calculation of mutations effect on Rv0678 dimer stability was performed using MMPBSA.py program within Amber14 suite. See materials and methods for details.

Figure S2. Heatmap of SNP based cluster analysis by distance matrix. The figure shows the SNP-based cluster analysis results of six MTBc strains groups harbouring the most frequent DLM-resistant related mutations. Colour scale in the square refers to the number of SNPs between each strain (12 SNPs threshold is reported from white to blue). The max number of SNPs are set to 15. MTBc lineages information is also reported.

Text S1. Supplementary material and methods. Supplementary information about protocols used for REMA and *in silico* analyses.

817 # Tables:

818 ## Table 1.

Gene locus	*Genomic coordinate* [a]	*Mutation (SNPs and Indels)* [b]	*BDQ MIC (µg/mL)* [c]	*Country* [d]	*Lineage (coll. lineage)*	*Treatment history* [e]	*DR pattern* [f]
Rv0678	779005	Gly6fs (Del_16-17 gg)	0.5	PAK	Delhi-CAS (3)	New	MDR, FQ-R
Rv0678-Rv0678	779016 779263	Gln9fs (Ins_27 c) Tyr92fs (Ins_274 a)	0.5	PAK	EAI (1,1,2)	Retreatment	MDR
Rv0678	779275	Arg96Trp (cgg/Tgg)	0.25	BGD	Delhi-CAS (3)	Retreatment	RIF, INH S
Rv0678	779321	Met111Lys (tag/aAg)	0.25	BGD	Haarlem (4,1,2,1)	New	RIF, INH S

819

820 ## Table 2.

Gene locus	*Genomic coordinate* [a]	*Mutation (SNPs and Indels)* [b]	*DLM MIC (µg/mL)* [c]	*Country* [d]	*Lineage (coll. Lineage)*	*Treatment history* [e]	*DR pattern* [f]
ddn	3986846	Met1fs (Del_2 t)	2	BGD	Eur-Amer.(4,1,2)	New	RIF, INH S
ddn	3986848	Pro2Gln (ccg/cAg)	0.25	AZE	mainly-T (4,8)	New	RIF, INH S
ddn	3986885	Ser14fs (Del_41 g)	> 4	BGD	Beijing (2,2,1)	Retreatment	MDR
ddn-fbiA	3986923 3640445	Trp27Stop (tgg/tAg) prom (g-18a)	> 4	BGD	EAI (1,1,3)	Retreatment	MDR
ddn	3986932	Arg30His (cgc/cAc)	1	BGD	EAI (1,1,3)	Retreatment	RIF, INH S
ddn	3986944	Gly34Glu (ggg/gAg)	0.12	AZE	LAM (4,3,3)	New	RIF, INH S
ddn	3987015	Gln58Stop (cag/Tag)	> 4	UKR	Beijing (2,2,1)	Retreatment	MDR, FQ-R
ddn-fbiA	3987025 3641164	Val61Gly (gtc/gGc) Ile208Val (atc/Gtc)	0.12	SA	Eur-Amer.(4,1,2)	New	RIF, INH S
ddn-fbiA	3987115 3640714	Asn91Thr (aac/aCc) Val58Ile (gtc/Atc)	0.25	AZE	mainly-T (4,8)	New	RIF, INH S
ddn	3987262	Thr140Ile (acc/aTc)	0.5	BGD	S-type (4,4,1,1)	New	RIF, INH S
fgd1	491723	Gly314Glu (gga/gAa)	0.12	BGD	Beijing (2,2,1)	New	RIF, INH S
fbiA	3640546	Lys2Glu (aag/Gag)	0.12	AZE	Beijing (2,2,1)	Retreatment	RIF, INH S
fbiA	3641002	Val154Ile (gta/Ata)	0.12	BGD	Beijing (2,2,1)	Retreatment	MDR, FQ-R
fbiA-fbiB	3641018 3642877	Pro159Gln (ccg/cAg) Lys448Arg (aag/aGg)	0.12	BGD	Delhi-CAS (3)	Retreatment	RIF, INH S
fbiA	3641164	Ile208Val (atc/Gtc)	0.25	BGD	Eur-Amer.(4,1,2)	New	RIF, INH S
fbiA	3641167	Ile209Val (atc/Gtc)	0.5	BGD	Eur-Amer.(4,5)	New	RIF, INH S
fbiA	3641403	Cys287Stop (tgc/tgA)	4	PAK	EAI (1,1,2)	New	RIF, INH S
fbiA	3641453	Arg304Gln (cgg/cAg)	0.25	PAK	Delhi-CAS (3)	New	MDR
fbiB	3642195	Gly221Ser (ggc/Agc)	0.12	BGD	Beijing (2,2,2)	New	FQ-R
fbiB	3642204	Asp224Asn (gac/Aac)	0.5	BGD	Delhi-CAS (3)	New	RIF, INH S
fbiB	3642351	Gly273Arg (ggc/Cgc)	0.25	BGD	X-Type (4,1,1,3)	New	RIF, INH S

fbiC	1303241	Tyr104Cys (tat/tGt)	0.5	AZE	Beijing (2,2,1)	Retreatment	RIF, INH S
fbiC	1303265	Gly112Ala (ggc/gCc)	0.12	BGD	EAI (1,1,3)	New	RIF, INH S
fbiC	1303612	Leu228Phe (ctc/Ttc)	0.12	BGD	EAI (1,1,3)	New	RIF, INH S
fbiC-fbiB	1303769 3642223	Ser280Leu (tcg/tTg) Arg230Gln (cgg/cAg)	0.12	BGD	EAI (1,1,3)	New	RIF, INH S
fbiC	1304498	Pro523Leu (cct/cTt)	0.5	BGD	EAI (1,1,3)	New	RIF, INH S
fbiC	1305101	Asn724Ser (aac/aGc)	0.25	BGD	Beijing (2,2,1)	New	RIF, INH S
fbiC	1305215	Ser762Asn (agc/aAc)	0.12	BGD	Delhi-CAS (3)	Retreatment	RIF, INH S; FQ-R
fbiC	1305434	Ala835Val (gcg/gTg)	0.5	BGD	EAI (1,1,3)	New	INH R
fbiC	1305494	Ala855fs (Del 62 nt)	0.5	SA	Haarlem (4,1,2,1)	New	RIF, INH S
fbiC-fbiB	1305494 3642874	Ala855fs (Del 62 nt) Leu447Arg (ctg/cGg)	0.25	SA	mainly-T (4,8)	Retreatment	MDR
fbiC	1305496	Ala856Pro (gcc/Ccc)	0.25	BGD	EAI (1,1,3)	New	RIF, INH S

Table S1

	locus name [a]	***genomic region*** [b]
Delamanid (DLM)	*fbiA_ups*	[3640142-3640542]
	fbiA (Rv3261)	[3640543-3641538]
	fbiB (Rv3262)	[3641535-3642881]
	fbiC_ups	[1302682-1302930]
	fbiC (Rv1173)	[1302931-1305501]
	fgd1_ups	[490683-490782]
	fgd1 (Rv0407)	[490783-491793]
	ddn_ups	[3986744-3986843]
	ddn (Rv3547)	[3986844-3987299]
Bedaquiline (BDQ)	*atpE_ups*	[1460997-1461044]
	atpE (Rv1305)	[1461045-1461290]
	Rv0678_ups	[778890-778989]
	Rv0678	[778990-779487]
	pepQ_ups	[2860419-2860518]
	pepQ (Rv2535)	[2859300-2860418]

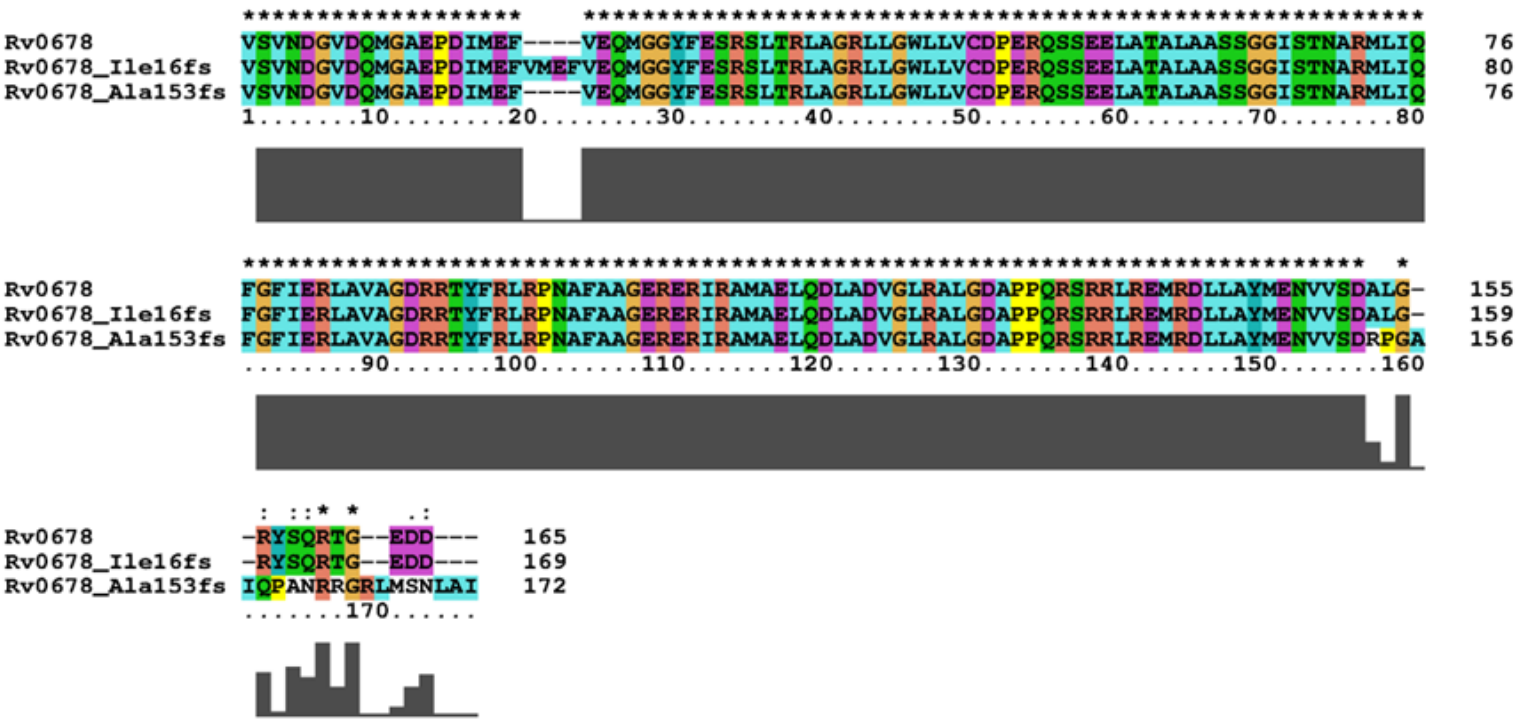
Rv0678 VSVNDGVDQMGAEPDIMEF----VEQMGGYFESRSLTRLAGRLLGWLLVCDPERQSSEELATALAASSGGISTNARMLIQ 76
Rv0678_Ile16fs VSVNDGVDQMGAEPDIMEFVMEFVEQMGGYFESRSLTRLAGRLLGWLLVCDPERQSSEELATALAASSGGISTNARMLIQ 80
Rv0678_Ala153fs VSVNDGVDQMGAEPDIMEF----VEQMGGYFESRSLTRLAGRLLGWLLVCDPERQSSEELATALAASSGGISTNARMLIQ 76
1.....10.....20.....30.....40.....50.....60.....70.....80
Rv0678 FGFIERLAVAGDRRTYFRLRPNAFAAGERERIRAMAELQDLADVGLRALGDAPPQRSRRLREMRDLLAYMENVVSDALG- 155
Rv0678_Ile16fs FGFIERLAVAGDRRTYFRLRPNAFAAGERERIRAMAELQDLADVGLRALGDAPPQRSRRLREMRDLLAYMENVVSDALG- 159
Rv0678_Ala153fs FGFIERLAVAGDRRTYFRLRPNAFAAGERERIRAMAELQDLADVGLRALGDAPPQRSRRLREMRDLLAYMENVVSDRPGA 156
.....90.....100.....110.....120.....130.....140.....150.....160
Rv0678 -RYSQRTG--EDD--- 165
Rv0678_Ile16fs -RYSQRTG--EDD--- 169
Rv0678_Ala153fs IQPANRRGRLMSNLAI 172
.....170.....

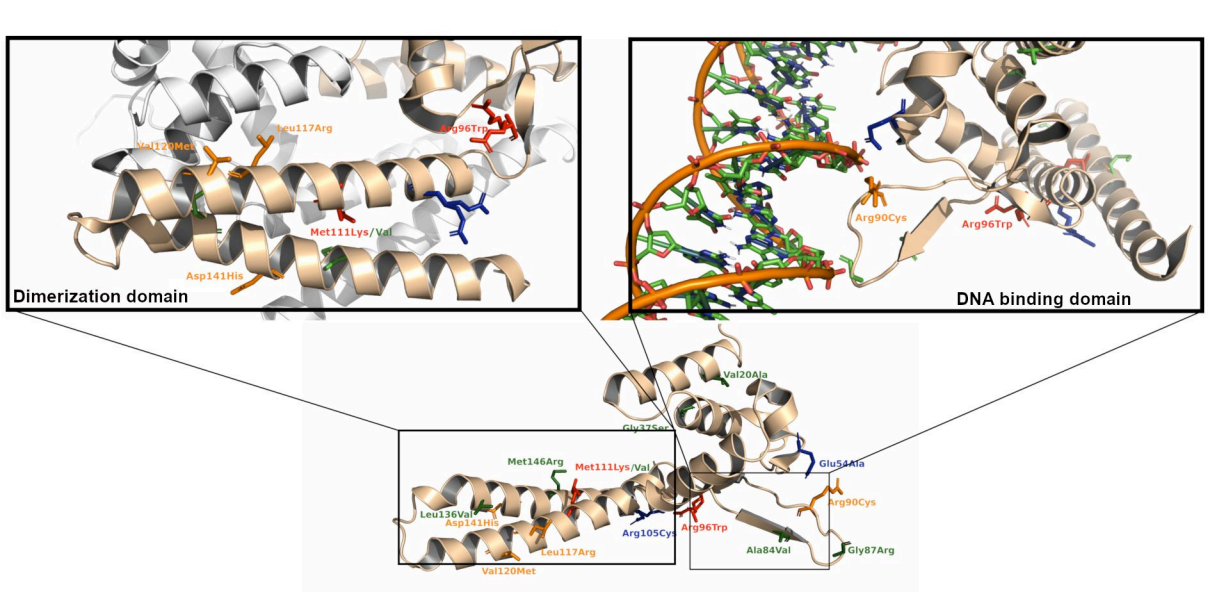
Dimerization domain
Leu117Arg
Arg96Trp
Val120Met
Met111Lys/Val
Asp141His
DNA binding domain
Arg90Cys
Arg96Trp
Val20Ala
Gly37Ser
Glu54Ala
Met146Arg
Met111Lys/Val
Arg90Cys
Leu136Val
Asp141His
Arg105Cys
Arg96Trp
Ala84Val
Gly87Arg
Leu117Arg
Val120Met

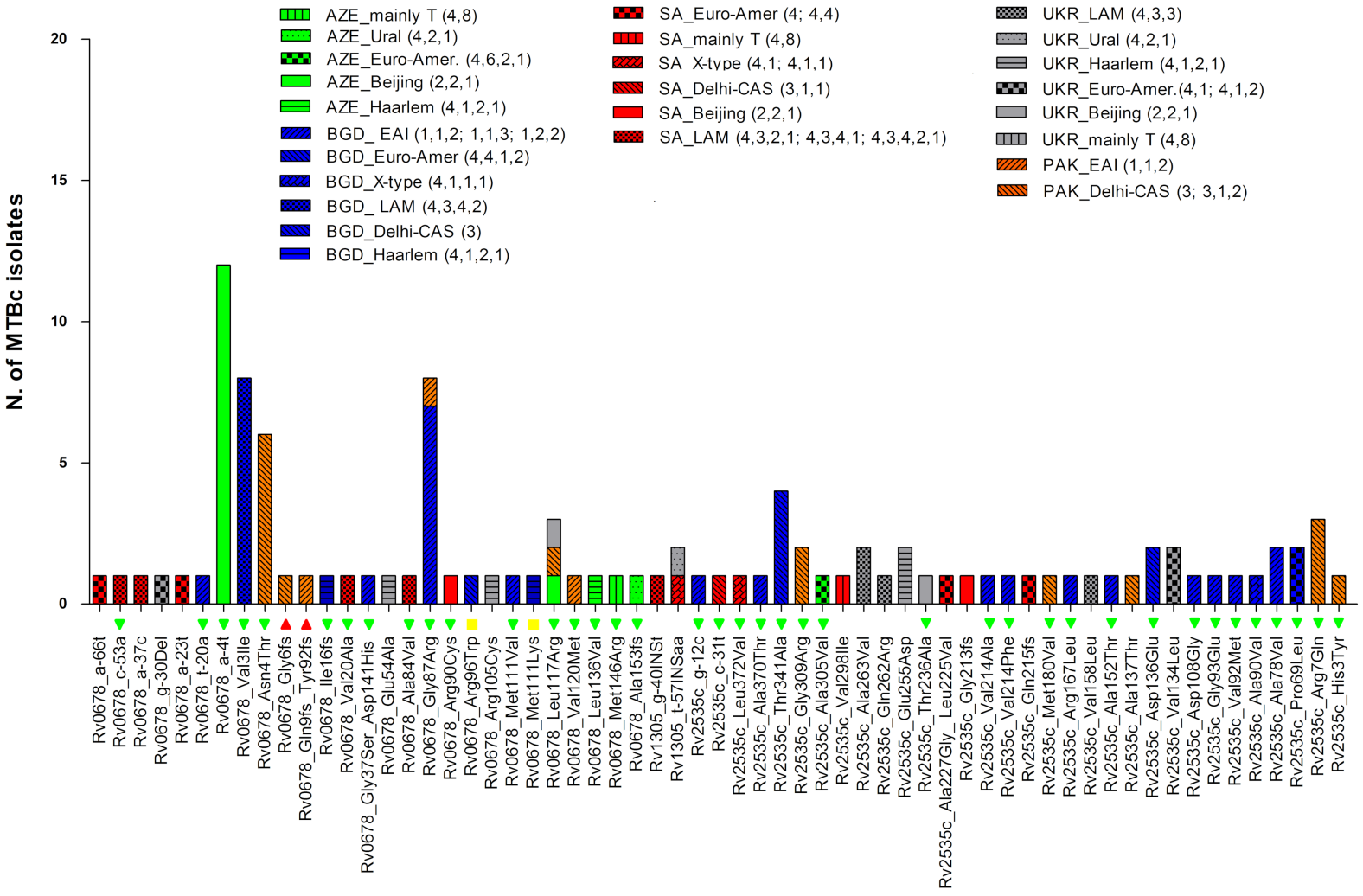
AZE_mainly T (4,8)
AZE_Ural (4,2,1)
AZE_Euro-Amer. (4,6,2,1)
AZE_Beijing (2,2,1)
AZE_Haarlem (4,1,2,1)
BGD_ EAI (1,1,2; 1,1,3; 1,2,2)
BGD_Euro-Amer (4,4,1,2)
BGD_X-type (4,1,1,1)
BGD_ LAM (4,3,4,2)
BGD_Delhi-CAS (3)
BGD_Haarlem (4,1,2,1)
SA_Euro-Amer (4; 4,4)
SA_mainly T (4,8)
SA_X-type (4,1; 4,1,1)
SA_Delhi-CAS (3,1,1)
SA_Beijing (2,2,1)
SA_LAM (4,3,2,1; 4,3,4,1; 4,3,4,2,1)
UKR_LAM (4,3,3)
UKR_Ural (4,2,1)
UKR_Haarlem (4,1,2,1)
UKR_Euro-Amer.(4,1; 4,1,2)
UKR_Beijing (2,2,1)
UKR_mainly T (4,8)
PAK_EAI (1,1,2)
PAK_Delhi-CAS (3; 3,1,2)
N. of MTBc isolates
20
15
10
5
0
Rv0678_a-66t
Rv0678_c-53a
Rv0678_a-37c
Rv0678_g-30Del
Rv0678_a-23t
Rv0678_t-20a
Rv0678_a-4t
Rv0678_Val3Ile
Rv0678_Asn4Thr
Rv0678_Gly6fs
Rv0678_Gln9fs_Tyr92fs
Rv0678_Ile16fs
Rv0678_Val20Ala
Rv0678_Gly37Ser_Asp141His
Rv0678_Glu54Ala
Rv0678_Ala84Val
Rv0678_Gly87Arg
Rv0678_Arg90Cys
Rv0678_Arg96Trp
Rv0678_Arg105Cys
Rv0678_Met111Val
Rv0678_Met111Lys
Rv0678_Leu117Arg
Rv0678_Val120Met
Rv0678_Leu136Val
Rv0678_Met146Arg
Rv0678_Ala153fs
Rv1305_g-40INSt
Rv1305_t-57INSaa
Rv2535c_g-12c
Rv2535c_c-31t
Rv2535c_Leu372Val
Rv2535c_Ala370Thr
Rv2535c_Thr341Ala
Rv2535c_Gly309Arg
Rv2535c_Ala305Val
Rv2535c_Val298Ile
Rv2535c_Ala263Val
Rv2535c_Gln262Arg
Rv2535c_Glu255Asp
Rv2535c_Thr236Ala
Rv2535c_Ala227Gly_ Leu225Val
Rv2535c_Gly213fs
Rv2535c_Val214Ala
Rv2535c_Val214Phe
Rv2535c_Gln215fs
Rv2535c_Met180Val
Rv2535c_Arg167Leu
Rv2535c_Val158Leu
Rv2535c_Ala152Thr
Rv2535c_Ala137Thr
Rv2535c_Asp136Glu
Rv2535c_Val134Leu
Rv2535c_Asp108Gly
Rv2535c_Gly93Glu
Rv2535c_Val92Met
Rv2535c_Ala90Val
Rv2535c_Ala78Val
Rv2535c_Pro69Leu
Rv2535c_Arg7Gln
Rv2535c_His3Tyr

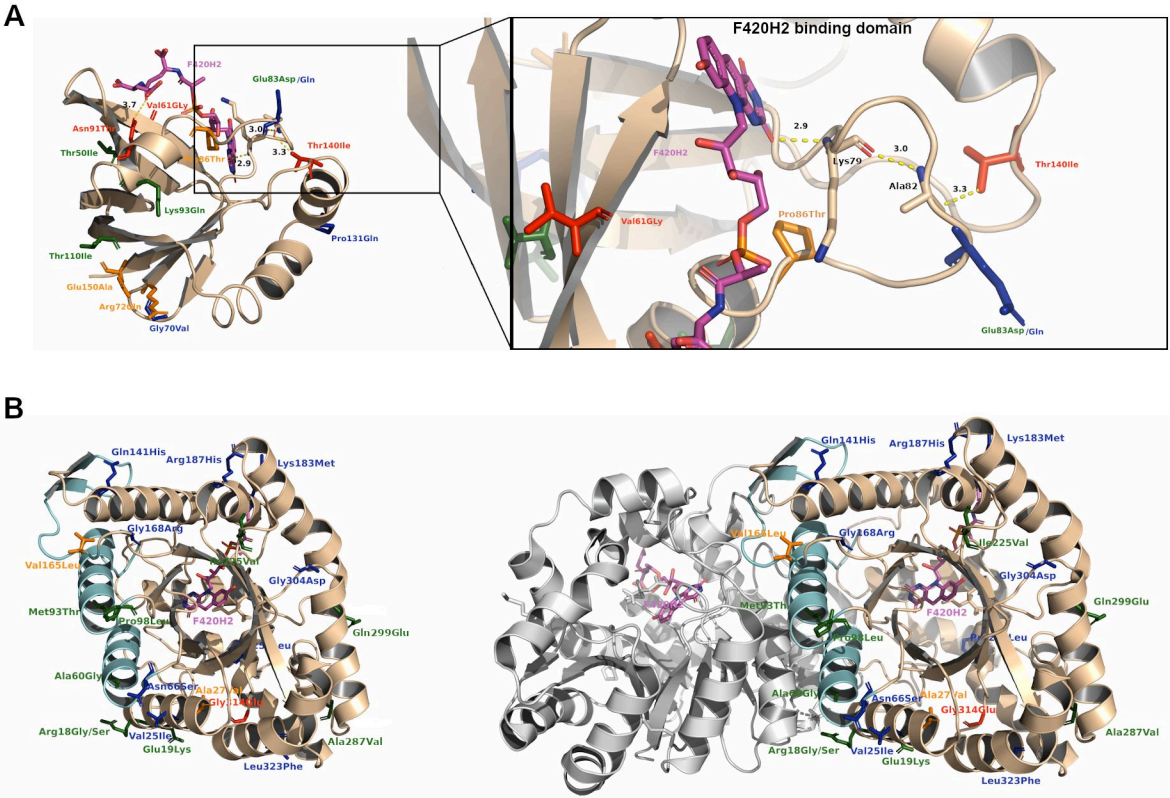
A
F420H2
Glu83Asp/Gln
Val61Gly
Asn91Thr
Thr50Ile
Pro86Thr
Thr140Ile
Lys93Gln
Pro131Gln
Thr110Ile
Glu150Ala
Arg72Gln
Gly70Val
F420H2 binding domain
Lys79
Ala82
Glu83Asp/Gln
B
Gln141His
Arg187His
Lys183Met
Gly168Arg
Val165Leu
Ile225Val
Gly304Asp
Met93Thr
Pro98Leu
F420H2
Gln299Glu
Ala60Gly
Asn66Ser
Ala27Val
Gly314Glu
Arg18Gly/Ser
Val25Ile
Glu19Lys
Ala287Val
Leu323Phe

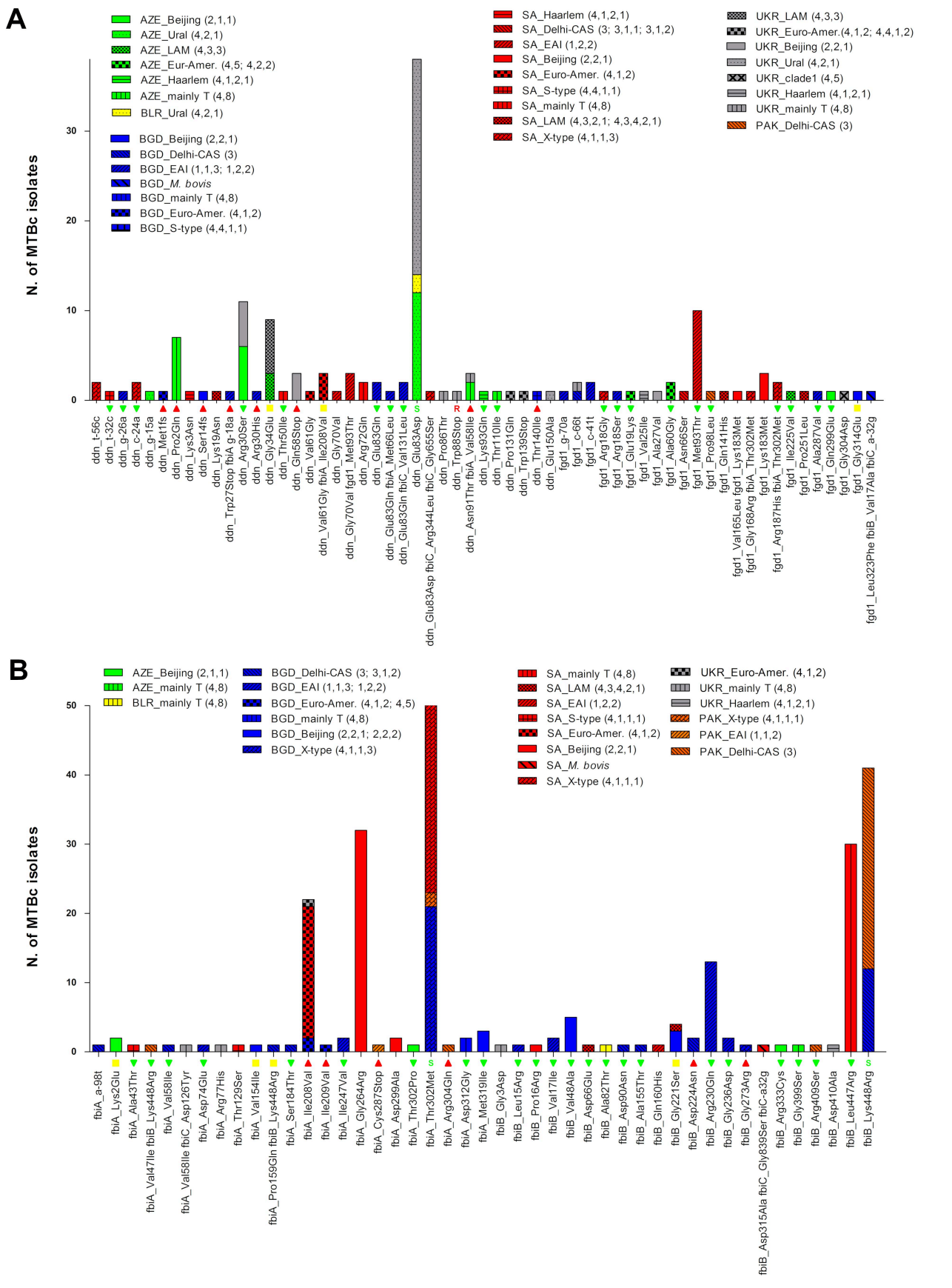
A
AZE_Beijing (2,1,1)
AZE_Ural (4,2,1)
AZE_LAM (4,3,3)
AZE_Eur-Amer. (4,5; 4,2,2)
AZE_Haarlem (4,1,2,1)
AZE_mainly T (4,8)
BLR_Ural (4,2,1)
BGD_Beijing (2,2,1)
BGD_Delhi-CAS (3)
BGD_EAI (1,1,3; 1,2,2)
BGD_M. bovis
BGD_mainly T (4,8)
BGD_Euro-Amer. (4,1,2)
BGD_S-type (4,4,1,1)
SA_Haarlem (4,1,2,1)
SA_Delhi-CAS (3; 3,1,1; 3,1,2)
SA_EAI (1,2,2)
SA_Beijing (2,2,1)
SA_Euro-Amer. (4,1,2)
SA_S-type (4,4,1,1)
SA_mainly T (4,8)
SA_LAM (4,3,2,1; 4,3,4,2,1)
SA_X-type (4,1,1,3)
UKR_LAM (4,3,3)
UKR_Euro-Amer.(4,1,2; 4,4,1,2)
UKR_Beijing (2,2,1)
UKR_Ural (4,2,1)
UKR_clade1 (4,5)
UKR_Haarlem (4,1,2,1)
UKR_mainly T (4,8)
PAK_Delhi-CAS (3)
N. of MTBc isolates
0
10
20
30
ddn_t-56c
ddn_t-32c
ddn_g-26a
ddn_c-24a
ddn_g-15a
ddn_Met1fs
ddn_Pro2Gln
ddn_Lys3Asn
ddn_Ser14fs
ddn_Lys19Asn
ddn_Trp27Stop fbiA g-18a
ddn_Arg30Ser
ddn_Arg30His
ddn_Gly34Glu
ddn_Thr50Ile
ddn_Gln58Stop
ddn_Val61Gly
ddn_Val61Gly fbiA_Ile208Val
ddn_Gly70Val
ddn_Gly70Val fgd1_Met93Thr
ddn_Arg72Gln
ddn_Glu83Gln
ddn_Glu83Gln fbiA_Met66Leu
ddn_Glu83Gln fbiC_Val131Leu
ddn_Glu83Asp
ddn_Glu83Asp fbiC_Arg344Leu fbiC_Gly655Ser
ddn_Pro86Thr
ddn_Trp88Stop
ddn_Asn91Thr fbiA_Val58Ile
ddn_Lys93Gln
ddn_Thr110Ile
ddn_Pro131Gln
ddn_Trp139Stop
ddn_Thr140Ile
ddn_Glu150Ala
fgd1_g-70a
fgd1_c-66t
fgd1_c-41t
fgd1_Arg18Gly
fgd1_Arg18Ser
fgd1_Glu19Lys
fgd1_Val25Ile
fgd1_Ala27Val
fgd1_Ala60Gly
fgd1_Asn66Ser
fgd1_Met93Thr
fgd1_Pro98Leu
fgd1_Gln141His
fgd1_Val165Leu fgd1_Lys183Met
fgd1_Gly168Arg fbiA_Thr302Met
fgd1_Lys183Met
fgd1_Arg187His fbiA_Thr302Met
fgd1_Ile225Val
fgd1_Pro251Leu
fgd1_Ala287Val
fgd1_Gln299Glu
fgd1_Gly304Asp
fgd1_Gly314Glu
fgd1_Leu323Phe fbiB_Val17Ala fbiC_a-32g
B
AZE_Beijing (2,1,1)
AZE_mainly T (4,8)
BLR_mainly T (4,8)
BGD_Delhi-CAS (3; 3,1,2)
BGD_EAI (1,1,3; 1,2,2)
BGD_Euro-Amer. (4,1,2; 4,5)
BGD_mainly T (4,8)
BGD_Beijing (2,2,1; 2,2,2)
BGD_X-type (4,1,1,3)
SA_mainly T (4,8)
SA_LAM (4,3,4,2,1)
SA_EAI (1,2,2)
SA_S-type (4,1,1,1)
SA_Euro-Amer. (4,1,2)
SA_Beijing (2,2,1)
SA_M. bovis
SA_X-type (4,1,1,1)
UKR_Euro-Amer. (4,1,2)
UKR_mainly T (4,8)
UKR_Haarlem (4,1,2,1)
PAK_X-type (4,1,1,1)
PAK_EAI (1,1,2)
PAK_Delhi-CAS (3)
N. of MTBc isolates
0
10
20
30
40
50
fbiA_a-98t
fbiA_Lys2Glu
fbiA_Ala43Thr
fbiA_Val47Ile fbiB_Lys448Arg
fbiA_Val58Ile
fbiA_Val58Ile fbiC_Asp126Tyr
fbiA_Asp74Glu
fbiA_Arg77His
fbiA_Thr129Ser
fbiA_Val154Ile
fbiA_Pro159Gln fbiB_Lys448Arg
fbiA_Ser184Thr
fbiA_Ile208Val
fbiA_Ile209Val
fbiA_Ile247Val
fbiA_Gly264Arg
fbiA_Cys287Stop
fbiA_Asp299Ala
fbiA_Thr302Pro
fbiA_Thr302Met
fbiA_Arg304Gln
fbiA_Asp312Gly
fbiA_Met319Ile
fbiB_Gly3Asp
fbiB_Leu15Arg
fbiB_Pro16Arg
fbiB_Val17Ile
fbiB_Val48Ala
fbiB_Asp66Glu
fbiB_Ala82Thr
fbiB_Asp90Asn
fbiB_Ala155Thr
fbiB_Gln160His
fbiB_Gly221Ser
fbiB_Asp224Asn
fbiB_Arg230Gln
fbiB_Gly236Asp
fbiB_Gly273Arg
fbiB_Asp315Ala fbiC_Gly839Ser fbiC-a32g
fbiB_Arg333Cys
fbiB_Gly399Ser
fbiB_Arg409Ser
fbiB_Asp410Ala
fbiB_Leu447Arg
fbiB_Lys448Arg

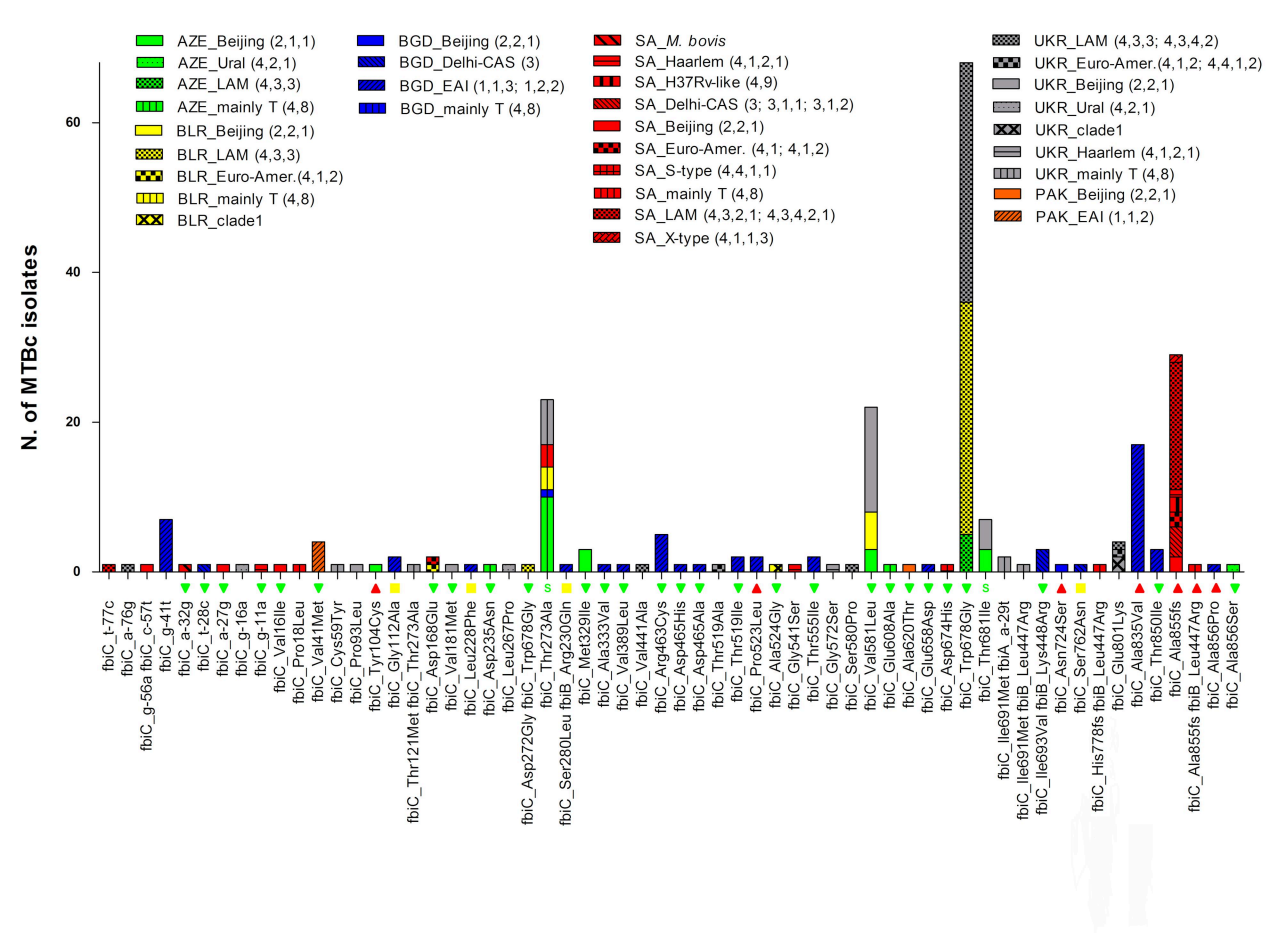
AZE_Beijing (2,1,1)
AZE_Ural (4,2,1)
AZE_LAM (4,3,3)
AZE_mainly T (4,8)
BLR_Beijing (2,2,1)
BLR_LAM (4,3,3)
BLR_Euro-Amer.(4,1,2)
BLR_mainly T (4,8)
BLR_clade1
BGD_Beijing (2,2,1)
BGD_Delhi-CAS (3)
BGD_EAI (1,1,3; 1,2,2)
BGD_mainly T (4,8)
SA_M. bovis
SA_Haarlem (4,1,2,1)
SA_H37Rv-like (4,9)
SA_Delhi-CAS (3; 3,1,1; 3,1,2)
SA_Beijing (2,2,1)
SA_Euro-Amer. (4,1; 4,1,2)
SA_S-type (4,4,1,1)
SA_mainly T (4,8)
SA_LAM (4,3,2,1; 4,3,4,2,1)
SA_X-type (4,1,1,3)
UKR_LAM (4,3,3; 4,3,4,2)
UKR_Euro-Amer.(4,1,2; 4,4,1,2)
UKR_Beijing (2,2,1)
UKR_Ural (4,2,1)
UKR_clade1
UKR_Haarlem (4,1,2,1)
UKR_mainly T (4,8)
PAK_Beijing (2,2,1)
PAK_EAI (1,1,2)
N. of MTBc isolates
0
20
40
60
fbiC_t-77c
fbiC_a-76g
fbiC_g-56a fbiC_c-57t
fbiC_g-41t
fbiC_a-32g
fbiC_t-28c
fbiC_a-27g
fbiC_g-16a
fbiC_g-11a
fbiC_Val16Ile
fbiC_Pro18Leu
fbiC_Val41Met
fbiC_Cys59Tyr
fbiC_Pro93Leu
fbiC_Tyr104Cys
fbiC_Gly112Ala
fbiC_Thr121Met fbiC_Thr273Ala
fbiC_Asp168Glu
fbiC_Val181Met
fbiC_Leu228Phe
fbiC_Asp235Asn
fbiC_Leu267Pro
fbiC_Asp272Gly fbiC_Trp678Gly
fbiC_Thr273Ala
fbiC_Ser280Leu fbiB_Arg230Gln
fbiC_Met329Ile
fbiC_Ala333Val
fbiC_Val389Leu
fbiC_Val441Ala
fbiC_Arg463Cys
fbiC_Asp465His
fbiC_Asp465Ala
fbiC_Thr519Ala
fbiC_Thr519Ile
fbiC_Pro523Leu
fbiC_Ala524Gly
fbiC_Gly541Ser
fbiC_Thr555Ile
fbiC_Gly572Ser
fbiC_Ser580Pro
fbiC_Val581Leu
fbiC_Glu608Ala
fbiC_Ala620Thr
fbiC_Glu656Asp
fbiC_Asp674His
fbiC_Trp678Gly
fbiC_Thr681Ile
fbiC_Ile691Met fbiA_a-29t
fbiC_Ile691Met fbiB_Leu447Arg
fbiC_Ile693Val fbiB_Lys448Arg
fbiC_Asn724Ser
fbiC_Ser762Asn
fbiC_His778fs fbiB_Leu447Arg
fbiC_Glu801Lys
fbiC_Ala835Val
fbiC_Thr850Ile
fbiC_Ala855fs
fbiC_Ala855fs fbiB_Leu447Arg
fbiC_Ala856Pro
fbiC_Ala856Ser